Published in final edited form as:
J Immunol. 2014 March 1; 192(5): 2480–2494. doi:10.4049/jimmunol.1302637.

Three tapasin docking sites in TAP cooperate to facilitate transporter stabilization and heterodimerization

Ralf M. Leonhardt[*,†], **Parwiz Abrahimi**[†], **Susan M. Mitchell**[†], and **Peter Cresswell**[*,†,‡]

[*]Howard Hughes Medical Institute, Yale University School of Medicine, 300 Cedar Street, New Haven CT 06520, USA

[†]Department of Immunobiology, Yale University School of Medicine, 300 Cedar Street, New Haven CT 06520, USA

[‡]Department of Cell Biology, Yale University School of Medicine, 300 Cedar Street, New Haven CT 06520, USA

Abstract

The transporter associated with antigen processing (TAP) translocates peptide antigens into the lumen of the endoplasmic reticulum (ER) for loading onto major histocompatibility complex (MHC) class I molecules. MHC class I acquires its peptide cargo in the peptide loading complex (PLC), an oligomeric complex that the chaperone tapasin organizes by bridging TAP to MHC class I and recruiting accessory molecules such as ERp57 and calreticulin. Three tapasin binding sites on TAP have been described, two of which are located in the N-terminal domains (N domains) of TAP1 and TAP2. The third binding site is present in the core transmembrane domain (coreTMD) of TAP1 and is only used by the unassembled subunits. Tapasin is required to promote TAP stability, but through which binding site(s) it is acting is unknown. In particular the role of tapasin binding to the coreTMD of TAP1 single chains is mysterious as this interaction is lost upon TAP2 association. In this study, we map the respective binding site in TAP1 to the polar face of the amphipathic transmembrane helix TM9 and identify key residues that are essential to establish the interaction. We find that this interaction is dispensable for the peptide transport function but essential to achieve full stability of human TAP1. The interaction is also required for proper heterodimerization of the transporter. Based on similar results obtained using TAP mutants lacking tapasin binding to either N domain, we conclude that all three tapasin-binding sites in TAP cooperate to achieve high transporter stability and efficient heterodimerization.

INTRODUCTION

Major histocompatibility complex (MHC) class I-mediated antigen presentation is a major pathway to eradicate tumors and virally infected cells in the body (1, 2). To this end, peptide antigens are generated in the cytosol mostly by the proteasome (3). These are then translocated into the endoplasmic reticulum (ER) by the peptide transporter associated with antigen processing (TAP) and loaded onto MHC class I molecules in the so-called peptide-loading complex (PLC) (4). The PLC is organized by the chaperone tapasin (5), which simultaneously binds TAP via its transmembrane domain (6–8) and MHC class I via its ER-lumenal domain (9). The function of the PLC is to facilitate the transfer of peptide antigens, typically 8–11 amino acids long, into the peptide binding groove of MHC class I and to edit the respective peptide repertoire in a way that only high affinity ligands are loaded (10–15).

Address correspondence to: Ralf M. Leonhardt, Ph.D., Yale University School of Medicine, Department of Immunobiology, 300 Cedar Street, TAC S669/670, New Haven, CT 06520-8011, USA, Tel. (203)-785-5042, Fax. (203)-785-4461; Ralf.Leonhardt@yale.edu.

Once MHC class I has captured an appropriate ligand, it dissociates from the PLC and migrates to the plasma membrane (1). Additional backup quality control mechanisms exist in case suboptimally loaded MHC class I molecules have been released from the ER (16–19). Peptide antigens are eventually presented at the cell surface to cytotoxic CD8-positive T cells, which can kill the target cells, if they recognize the peptide as abnormal or of nonself origin (2).

TAP is a member of the ATP-binding cassette (ABC) transporter family (4). The molecule forms a heterodimer consisting of two subunits, TAP1 and TAP2, and resides in the ER membrane where it shuttles peptides from the cytosol into the ER (4). Both TAP subunits have a similar domain structure, in which an N-terminal transmembrane domain (TMD) is followed by a cytosolic C-terminal nucleotide binding domain (NBD) (Fig. 1A). The NBD selects and hydrolyzes nucleotides to energize the transport cycle (4, 20). The TMD can be further subdivided into an N-terminal domain (N domain), containing four membrane-spanning segments in TAP1 and three membrane-spanning segments in TAP2, and a central core transmembrane domain (coreTMD) containing six transmembrane helices (Fig. 1A and (21)). The coreTMD binds the peptide ligands and forms the translocation pore (4). The N domains in both TAP1 and TAP2 are not essential for peptide transport, but each contains one single independent docking site for tapasin (18, 22–24). Hence, within the PLC each assembled TAP1:TAP2 heterodimer interacts with two molecules of tapasin (18, 22, 25, 26). For both these interactions, tapasin uses its single transmembrane segment (7, 8), which has been reported to associate with the first membrane-spanning helix in the N domain of TAP1 and TAP2 (6). Recently, a third tapasin binding site was described that is located within the coreTMD of TAP1 (18). This binding site, however, appears only to be accessible in unassembled TAP1 chains but not in assembled TAP, indicating that TAP2 and tapasin may compete for binding to an overlapping surface area of the molecule (18). In contrast, no tapasin binding was detected to the coreTMD of TAP2 (18).

Besides the formation of the PLC, the interaction between TAP and tapasin serves another major purpose, to stabilize the transporter. In human cells lacking tapasin, TAP levels may be 3 to >10-fold reduced, while studies on tapasin-deficient murine cells reported >100-fold lower TAP levels than in wildtype cells (7–9, 27, 28). However, it is unknown whether tapasin causes higher steady state levels of TAP via binding to the N domain of TAP1, the N domain of TAP2, or the coreTMD of unassembled TAP1 prior to transporter heterodimerization. In fact, all these interactions could be necessary to achieve full TAP stability. Moreover, the tapasin docking site in the coreTMD of TAP1 has not been characterized and it is unclear whether it serves a function in transporter assembly and/or stability. To address these issues, we performed extensive mutagenesis on the coreTMD of TAP1 and identified the transmembrane segment TM9 as the tapasin binding site in this domain. TM9 forms an amphipathic alpha-helix and we find the polar face of this segment to be essential for tapasin association. Within this polar face we identify six critical amino acids that if mutated abrogate tapasin binding. Strikingly, despite being functional TAP1 chains, the tapasin binding mutants display poor heterodimerization with TAP2, suggesting that the interaction of tapasin with the coreTMD of TAP1 may be necessary for proper TAP assembly. Moreover, docking of tapasin to both the N domain and the coreTMD of unassembled TAP1 is required for full stability of the subunit: eliminating either binding site alone has only a small effect but mutating both simultaneously causes a drastic reduction in stability. Further analysis of N-terminal deletion mutants of both TAP1 and TAP2 suggest that all three tapasin binding sites may cooperate to facilitate assembly of the intact transporter.

MATERIALS AND METHODS

Cell lines and cell culture

T2 is a human lymphoblastoid cell line expressing HLA-A2 and HLA-B51 (29). Untransfected T2 cells or transfectants of T2 expressing wt-TAP1 or TAP1 mutants were cultured in Iscove's modified Dulbecco's medium (Sigma), 10% FCS (HyClone) containing non-essential amino acids (Invitrogen), GlutaMax (Invitrogen), and penicillin/streptomycin (Invitrogen). T2 cells expressing wt-TAP2 or TAP2 mutants were grown in medium additionally containing 2 mg/ml G418 (Gibco). T2 cells co-expressing wt-TAP1 and wt-TAP2, 1ΔN and wt-TAP2, or wt-TAP1 and 2ΔN have been described previously (25).

Antibodies

R.SinE (30), R.RING4C (31), and R.gp48N (5) are rabbit polyclonal antibodies raised against soluble recombinant tapasin, the C-terminus of TAP1, and the N-terminus of tapasin, respectively. 3H6, a mouse monoclonal antibody raised against tapasin, was a kind gift from Dr. Jim McCluskey. 148.3 (32), K0137-3 (MBL International), PaSta-1 (33), HC-10 (34), and 4E (35) are mouse monoclonal antibodies recognizing TAP1 (C-terminus), TAP2, tapasin, free HLA-B and HLA-C heavy chains, and folded, β_2-microglobulin-associated HLA-B and HLA-C molecules, respectively. The mouse monoclonal antibody 435.3 (36) also recognizes TAP2. 9G10 (Enzo Life Sciences) is a rat monoclonal antibody recognizing Grp94.

Vector constructs and TAP expression

Constructs TAP2 or 2ΔN in pLNCX2 and TAP1 or 1ΔN in pLPCX have been described previously (25). For generation of construct 1ΔN-TM5, first the TAP1 TM5 was deleted from vector 1ΔN in pLPCX using a standard QuikChange mutagenesis with primer pair 5'-CGGAGACGCGCCGGCTCACTGACTGGATTC-3'/5'-GAATCCAGTCAGTGAGCCGGCGCGTCTCCG-3'. Next, primers 5'-TCGCCGGCTCGTTGCCGCCTTCTTCTTCCTTGTCCTTGCTGTCTTGGGTGAG-3' and 5'-AAGCCGGCCCGTATAGTGAGGGATTAATGTCTCACCCAAGACAGCAAGGAC-3' were annealed and a DNA fragment encoding the TAP2-TM4 was synthesized in a Taq-driven primer extension reaction. Finally, the NgoM IV-flanked TM4 was cloned into the NgoM IV site in the 1ΔN deletion variant described above. For generation of construct 1ΔN-TM6, TAP1/TAP2-hybrid primers 5'-TGGCTCAGCCGATACCTTCACTCGAAACATCTTCTTCATGTGCCTCTTCTCC-3' and 5'-TTCACGTGGCCCATTGTGTTGTTATAGCAGCCTCCTCGGCAGCCT-3' were used to amplify the TAP2 TM5 in a standard Taq-driven PCR using a TAP2-containing vector as template. This fragment was cleaved with Blp I and Pml I and ligated into Blp I/Pml I-cleaved 1ΔN in pLPCX. For generation of construct 1ΔN-TM9, three sequential QuikChange mutagenesis steps were performed beginning with 1ΔN in pLPCX as a template: Mutagenesis with primers 9/1F and 9/1B (see supplementary Table S1 for all QuikChange primer sequences) exchanged roughly the first third of the TAP1 TM9 to the respective residues in TAP2 TM8, resulting in construct 1ΔN-TM9/1 (see Fig. 4A/B). Using 1ΔN-TM9/1 as a template, mutagenesis with primers 9/2F and 9/2B additionally exchanged the second third of the TAP1 TM9 against the respective residues in TAP2, resulting in construct 1ΔN-TM9/2 (see Fig. 4A/B). Finally, using 1ΔN-TM9/2 as a template, mutagenesis with primer pair TM9F/TM9B resulted in construct 1ΔN-TM9, in which the entire TAP1 TM9 is exchanged to the respective residues from TAP2 TM8. An analogous strategy was followed to generate constructs 1ΔN-TM7, 1ΔN-TM8, and 1ΔN-TM10, using a three-step QuikChange mutagenesis protocol with primers 7/1F, 7/1B, 7/2F, 7/2B, TM7F, TM7B, and 8/1F, 8/1B, 8/2F, 8/2B, TM8F, TM8B, and 10/1F, 10/1B, 10/2F, 10/2B, TM10F,

TM10B, respectively. All TAP1 mutant and wildtype derivatives described above that were later transduced into T2 cells were ligated into the Xho I/Not I sites of the retroviral vector pBMN-IRES-EGFP as Xho I/Not I fragments. Constructs 1ΔN-R_1Q, 1ΔN-R_2Q, 1ΔN-N411Y, 1ΔN-N411K, 1ΔN-N411A, 1ΔN-T415Q, 1ΔN-T415A, 1ΔN-G419A, and 1ΔN-G419H were generated by QuikChange mutagenesis using 1ΔN in pBMN-IRES-EGFP as template vector in combination with primer pairs R_1QF/R_1QB, R_2QF/R_2QB, N411YF/N411YB, N411KF/N411KB, N411AF/N411AB, T415QF/T415QB, T415AF/T415AB, G419AF/G419AB, and G419HF/G419HB, respectively. Construct 1ΔN-K423Q* in pBMN-IRES-EGFP was an accidental product generated via QuikChange mutagenesis using above mentioned primer pair R_1QF/R_1QB but contained the additional unwanted mutation M202I. The latter unwanted mutation was removed by swapping sequences between 1ΔN and 1ΔN-K423Q* to give rise to construct 1ΔN-K423Q in pBMN-IRES-EGFP. Constructs 1ΔN-RHQ and 1ΔN-LYLLVRQ were generated by QuikChange mutagenesis using 1ΔN-R_1Q in pBMN-IRES-EGFP as template vector in combination with primer pairs RHQF/RHQB and LYLLVRQF/LYLLVRQB. Constructs 1ΔN-YRHQ, 1ΔN-YLRHQ_1, and 1ΔN-LRHQ were generated by QuikChange mutagenesis using 1ΔN-RHQ in pBMN-IRES-EGFP as template vector in combination with primer pairs YRHQF/YRHQB, YLRHQ_1F/YLRHQ_1B, and LRHQF/LRHQB, respectively. Constructs 1ΔN-YVRHQ, 1ΔN-YLRHQ_2, and 1ΔN-YLVRHQ were generated by QuikChange mutagenesis using 1ΔN-YRHQ in pBMN-IRES-EGFP as template vector in combination with primer pairs YVRHQF/YVRHQB, YLRHQ_2F/YLRHQ_2B, and YLVRHQF/YLVRHQB, respectively. Constructs 1ΔN-3AQ and 1ΔN-5AQ were generated by QuikChange mutagenesis using 1ΔN-K423Q in pBMN-IRES-EGFP as template vector in combination with primer pairs 3AQF/3AQB and 5AQF/5AQB, respectively. Constructs TAP1-3AQ and TAP1-5AQ were generated by ligating the 1296 bp Xcm I/Xcm I fragment derived from 1ΔN-3AQ and 1ΔN-5AQ, respectively, into Xcm I-cleaved TAP1 in pBMN-IRES-EGFP thereby replacing the corresponding 1296 bp segment in full-length TAP1.

All vectors containing mutant or wildtype TAP1 (in pBMN-IRES-EGFP) or TAP2 (in pLNCX2) were sequenced in both directions before retroviral transduction into T2 cells (37). A detailed transduction protocol can be found at Leonhardt et al (38). T2 transfectants expressing TAP1 derivatives were either sorted twice for EGFP expression or cloned by limiting dilution or both in order to obtain a TAP-positive population. T2 transfectants expressing TAP2 derivatives were selected in medium containing 2 mg/ml G418 (Gibco) and cloned by limiting dilution.

Immunofluorescence, flow cytometry, and Western blotting

Immunofluorescence microscopy was performed as described (39). Briefly, T2 transfectants were washed with PBS and fixed with 2% formaldehyde (15 min at room temperature (RT)). After quenching with PBS/ 10 mM glycine followed by a wash with PBS/ 0.5% BSA, the cells were permeabilized for 1h in staining buffer (PBS/ 0.5% BSA/ 0.5% saponin) and stained for 1h with the TAP1-specific antibody 148.3 (1:100) in staining buffer. Antibody 148.3 has been used in immunofluorescence applications before (40). After three washes with staining buffer, an Alexa647-conjugated goat-anti-mouse IgG secondary antibody (Molecular Probes) was applied at a 1 : 100 dilution in the same buffer, before cells were washed again three times, mounted in ProLong Gold reagent (Invitrogen) and analyzed by confocal fluorescence microscopy using a Leica TCS SP2 Confocal Microscope (Leica Microsystems).

Flow cytometry was performed as described (40), using the antibody 4E directly conjugated to Alexa647 at a concentration of 1 : 30. Live-cell gating was performed using YO-PRO-1 iodide (Invitrogen) or propidium iodide (Sigma). All data were acquired on a FACSCalibur flow cytometer (BD Biosciences) and analyzed using FlowJo 6.4.7 software (Tree Star).

Western blotting was carried out as described (26). Importantly, because TAP1 and TAP2 are multi-spanning membrane proteins, lysates were not boiled to avoid aggregation but vortexed for 30 min at RT for denaturation.

Pulse-chase analysis and immunoprecipitation

Radiolabeling was performed as described (41). Briefly, 2.2×10^7 starved T2 cells expressing individual TAP1 subunits or heterodimeric TAP transporter derivatives were pulse-labeled at 37 °C with [^{35}S]methionine/cysteine (PerkinElmer Life Sciences) at 0.5 mCi/ml in 2.2 ml for 1 h and subsequently chased in Iscove's modified Dulbecco's medium, 10% FCS containing an excess of cold L-methionine/L-cysteine (both at 0.45 mg/ml) for up to 8 h. Following this, cells were harvested and frozen at −80 °C until the next day or immediately lysed in 1% digitonin (Calbiochem) (containing protease inhibitor mixture (Roche Applied Science)) at 10^7 cells/ml and pre-cleared overnight using protein A.

For immunoprecipitation, antibody 148.3-coupled protein A-Sepharose was used. If the pre-clear had not been performed overnight, the frozen cell pellets were thawed, lysed in 1% digitonin (Calbiochem) (containing protease inhibitor mixture (Roche)) at 10^7 cells/ml, and pre-cleared using protein A-Sepharose beads. Subsequently, the supernatant was applied to 148.3-coupled beads and immunoprecipitation was carried out as described (19). Briefly, supernatants were incubated with antibody-coupled beads for 2 h at 4 °C on a rotator and washed five times with PBS/ 0.1% digitonin before bound proteins were eluted by vortexing in 100 mM Tris/ 0.5% SDS for 30 min at RT. Because TAP1 and TAP2 are multi-spanning membrane proteins, immunoprecipitates were not boiled in SDS sample buffer to avoid aggregation but vortexed for 30 min at RT for denaturation. After separation of immunoprecipitates by SDS-PAGE, gels were dried, exposed to PhosphorImager screens, and analyzed with ImageQuant 5.2 (GE Healthcare). Immunoprecipitations from non-radioactively labeled cells were carried out analogously after lysis of 10^7 cells in 1 ml of PBS/ 1% digitonin (Calbiochem) (containing protease inhibitor mixture (Roche)) if not otherwise indicated.

RT-PCR

Total RNA was extracted from T2 transfectants using the RNeasy Mini Kit (Qiagen) and cDNA was prepared using the First Strand Synthesis Kit (Stratagene). Actin-specific primers have been described (39). To detect TAP2, the primer pair 5'-ACCCTGATGAGTAACTGGCTTCC-3'/5'-CCCAAAACTGCGAACGGTCTGC-3' was used to amplify a 267 bp fragment in a standard Taq-driven PCR (annealing temperature 60 °C / 35 cycles)

RESULTS

The core transmembrane domain of unassembled human TAP1 contains a tapasin binding site that involves transmembrane segment TM9

Tapasin interacts with both the human and the rat assembled antigenic peptide transporter TAP via the N-terminal domains (N domains) of TAP1 and TAP2 (18, 23, 24). In addition, unassembled rat TAP1 subunits, but not rat TAP2 subunits, can interact with human tapasin via their core transmembrane domain (coreTMD), but this interaction is lost once the transporter chain heterodimerizes with TAP2 (18). The nature of this interaction remains undefined. It is also well established that tapasin substantially stabilizes TAP, allowing significantly higher levels of TAP protein to accumulate in the cell (7–9, 27, 28, 42). However, whether tapasin promotes TAP stability through binding to the N domains of TAP2 and TAP1 or through binding to the coreTMD of unassembled TAP1 or through all of these interactions is unknown. To address these issues, we aimed to construct a mutant

TAP1 subunit lacking the tapasin binding site within the coreTMD and analyze its capability to restore TAP function and MHC class I-mediated antigen presentation in TAP-deficient T2 cells.

Because this interaction had so far only been described to occur between rat TAP1 and human tapasin in a hybrid experimental system (18), we first examined whether it could also be observed in a purely human system. To this end, we generated a functional human N-terminal deletion mutant of TAP1 (Δ2–162) lacking the N domain but retaining the coreTMD (25), referred to as 1ΔN (Fig. 1A/B). To assess whether this construct can interact with tapasin, we generated stable clones of the human TAP-deficient cell line T2 expressing either full-length wildtype TAP1 or 1ΔN and performed an immunoprecipitation from digitonin lysates with either TAP1-specific (148.3) or tapasin-specific (PaSta-1) antibodies. As shown in Fig. 1C/D, 1ΔN clearly associated with tapasin, although to a lower extent than wt-TAP1.

Tapasin has been reported to use its single transmembrane segment to associate with the first transmembrane helix of both N domains in TAP (6–8). We therefore speculated that the interaction between the chaperone and the coreTMD of unassembled TAP1 might also involve transmembrane segments. Recently, the topology of TAP1 and, in particular, the positions of the transmembrane helices within TAP1 had been determined (21). Because previous studies had indicated that only unassembled TAP1 but not unassembled TAP2 associates with tapasin via the coreTMD (18), we exchanged each of the six transmembrane helices (TM5 through TM10) in the coreTMD of 1ΔN individually to the respective sequence counterpart of the collinear TAP2 molecule (Fig. 2A). This strategy gave rise to six different 1ΔN variants, 1ΔN-TM5 through 1ΔN-TM10, in each of which one transmembrane segment was replaced by the corresponding TAP2-derived sequence (Fig. 2B). All these mutants were stably expressed in T2 cells and analyzed by Western blotting. 1ΔN-TM9 could be expressed at normal levels when compared to the parental 1ΔN construct, 1ΔN-TM5 at somewhat reduced levels, and the other four constructs (1ΔN-TM6, 1ΔN-TM7, 1ΔN-TM8, and 1ΔN-TM10) only at very low levels (*data not shown*). To determine whether these mutants were capable of interacting with tapasin, we immunoprecipitated them with the anti-TAP1 monoclonal antibody 148.3 from digitonin lysates and assessed the co-precipitation of tapasin (Fig. 2C–G). Constructs 1ΔN-TM5 and 1ΔN-TM7, although expressed at reduced levels, efficiently co-isolated tapasin at near normal levels when normalized to immunoprecipitated 1ΔN (Fig. 2C/E), indicating that TM5 and TM7 are not involved in tapasin binding. Construct 1ΔN-TM8 also bound tapasin even though the interaction appeared substantially diminished (Fig. 2F). Constructs 1ΔN-TM6 and 1ΔN-TM10 displayed no tapasin binding at all (Fig. 2D/F), but given the very low expression levels of these mutants even in clones selected for highest expression (*data not shown*), these results may reflect folding issues rather than the loss of a specific interaction. Strikingly, though, construct 1ΔN-TM9, which was expressed at levels equal to or higher than the parental 1ΔN, completely lacked tapasin binding (Fig. 2G). Next, we compared the subcellular distribution of 1ΔN-TM9 and 1ΔN by confocal immunofluorescence microscopy and for both constructs we observed an identical reticular staining pattern with additional labeling surrounding the nucleus, demonstrating that both mutants properly localized to the endoplasmic reticulum (ER) (Fig. 3A). This indicates that loss of tapasin binding by 1ΔN-TM9 did not reflect a loss of ER retention.

One major advantage of exchanging transmembrane segments between TAP2 and TAP1 rather than using TAP1 deletion constructs is that the respective mutants may retain function, which would indicate that they are properly folded and hence that loss of tapasin binding is not a result of major structural defects. To assess whether 1ΔN-TM9 is functional, we transduced the respective T2 transfectant with TAP2 to determine whether

heterodimerization occurred. Indeed, when 1ΔN-TM9 was immunoprecipitated with TAP1-specific antibodies, TAP2 was co-isolated, indicating that this mutant subunit was able to associate with TAP2 (Fig. 3B). Moreover, in a functional flow cytometry assay, monitoring the ability of the 1ΔN-TM9/TAP2 transporter to promote the surface expression of the TAP-dependent molecule HLA-B*5101, we observed an HLA-B,C-positive population after TAP2 transduction into cells pre-expressing 1ΔN-TM9 (Fig. 3C/D) (this experiment was performed prior to selection for TAP2 expressing cells, and the two peaks in the FACS histograms in Fig. 3C likely reflect the presence of TAP2-positive and TAP2-negative cells). Hence, construct 1ΔN-TM9 retains to a significant extent the ability to associate with TAP2 and generate a functional transporter, suggesting that loss of tapasin binding in this mutant reflects the loss of a specific interaction site and not major misfolding.

Tapasin binding via the coreTMD of TAP1 involves the contribution of six key amino acids on the polar face of the amphipathic transmembrane segment TM9

Having established TM9 as the major site for tapasin docking to the coreTMD of TAP1, we attempted to map the interaction to individual amino acid residues within the transmembrane helix. To this end, we first generated three constructs, in which only the first third (1ΔN-TM9/1), only the first two thirds (1ΔN-TM9/2), or the entire TM9 (1ΔN-TM9) were exchanged for the respective sequences from TAP2 (Fig. 4A/B). Construct 1ΔN-TM9/2 could be expressed at high levels in the cell, while 1ΔN-TM9/1 was expressed only to a very low extent (Fig. 4C). This is probably due to the fact that 1ΔN-TM9/1 contains three positively charged residues in transmembrane segment TM9 (Arg-415, Arg-416, Lys-423), whereas 1ΔN-TM9/2 contains only two (Arg-415, Arg-416) (Fig. 4A), perhaps allowing better accommodation of the segment into the membrane bilayer. Interestingly, neither construct interacted with tapasin (Fig. 4D), although they were retained in the ER (Fig. 4E), suggesting that it is the identity of the N-terminus of the TAP1 TM9 that is important for tapasin binding.

The TAP2 transmembrane segment TM8 (as given in the Swiss Protein data base (21)), which corresponds to TAP1 transmembrane segment TM9 (Fig. 1A), contains a prominent pair of positively charged arginine residues in its N-terminal third (Fig. 4A). Thus, it was tempting to speculate that the introduction of these basic residues disrupted tapasin binding in constructs 1ΔN-TM9, 1ΔN-TM9/1, and 1ΔN-TM9/2. To test this hypothesis we mutated the respective residues, Thr-415 and Ser-416, to arginine individually. Additionally, given our experience with construct 1ΔN-TM9/1, which suggested that the simultaneous presence of basic residues in the N-terminal and in the middle segments of TM9 may cause poor expression, we neutralized Lys-423 by changing it to the glutamine found in TAP2 (Fig. 4F). This strategy allowed the successful expression of high levels of three constructs, containing arginine at position 415 (1ΔN-R_1Q), 416 (1ΔN-R_2Q), or at none of the two positions (1ΔN-K423Q*) (Fig. 4F/G). Interestingly, the K423Q exchange alone appeared to result in weaker tapasin binding as shown by slightly reduced co-precipitation of the chaperone when compared to 1ΔN, particularly when levels of co-isolated tapasin were normalized to levels of precipitated 1ΔN (Fig. 4H, *lane 3*). The additional introduction of arginine at position 415 (in 1ΔN-R_1Q) but not at position 416 (in 1ΔN-R_2Q) further reduced tapasin binding (Fig. 4H, *lanes 4 and 5*), indicating that Thr-415 and Lys-423 contribute to the interaction (Fig. 4J, *see red asterisks in helical wheel model of TM9*). Although tapasin association with construct 1ΔN-R_1Q was clearly diminished (Fig. 4H) substantial residual binding could still be detected. We therefore aimed to introduce additional mutations abrogating this binding activity. To this end, we generated two constructs, which were both based on the mutant 1ΔN-R_1Q. In the first, all TM9 residues N-terminal to Thr-415 (residues 410–414) were exchanged to their counterparts in TAP2 giving rise to construct 1ΔN-LYLLVRQ (Fig. 4I). This construct represents a variant of the poorly expressed 1ΔN-

TM9/1 not containing the mutation at residue 416, which our results in Fig. 4H had already shown to be dispensable for tapasin binding. However, very likely due to the neutralization of residue Lys-423, construct 1ΔN-LYLLVRQ could be expressed at much higher levels than 1ΔN-TM9/1 (Fig. 4K, *lane 4*). Interestingly, construct 1ΔN-LYLLVRQ displayed a drastic reduction in tapasin binding when compared to the parental construct 1ΔN-R_1Q (Fig. 4L, *lanes 3 and 4*), suggesting that the first N-terminal third of the TM9 plays a key role in the interaction. Furthermore, we generated a second mutant, 1ΔN-RHQ, also based on construct 1ΔN-R_1Q, in which we additionally exchanged Gly-419 to the histidine found in TAP2 (Fig. 4I). Gly-419 was chosen because it lay between critical residues Thr-415 and Lys-423 in both the primary amino acid sequence (Fig. 4I) and in the helical wheel projection of TM9 (Fig. 4J). 1ΔN-RHQ was also expressed well (Fig. 4K) and the G419H mutation did substantially affect tapasin association (Fig. 4L, *lanes 3 and 5*), suggesting a possible role for Gly-419 in the binding.

Next, we focused on the role of residues in the first N-terminal third of TM9. We started with construct 1ΔN-RHQ and additionally exchanged either Asn-411 or Trp-413 or both to their corresponding residues in TAP2 (tyrosine and leucine, respectively) (Fig. 5A). All these mutants were well expressed (Fig. 5B) and the additional N411Y mutation almost completely abrogated tapasin binding (Fig. 5C, *see 1ΔN-YRHQ and 1ΔN-YLRHQ$_1$*). In contrast, mutation of the highly conserved Try-413 did not affect the tapasin interaction at all (Fig. 5C, *compare lanes 4 and 6*). Taken together, the combined alteration in construct 1ΔN-YRHQ of four amino acids in the TAP1 transmembrane segment TM9 - N411Y, T415R, G419H, and K423Q - almost eliminated tapasin association.

Finally, in an attempt to totally eliminate tapasin binding we additionally exchanged residues Ser-412 or Thr-414 in 1ΔN-YRHQ, or both, to their corresponding residues in TAP2 (leucine and valine, respectively) (Fig. 5D/E). Individually these exchanges had only little impact on tapasin binding, but the combined exchange in construct 1ΔN-YLVRHQ completely abrogated any residual interaction (Fig. 5F, *lane 7*). When projected onto a helical wheel, the N-terminal two thirds of the TAP1 TM9 display pronounced amphipathicity with hydrophobic amino acids on one face and mostly polar and one charged amino acid on the other face (Fig. 5I). In contrast, the corresponding transmembrane segment in TAP2 is less amphipathic and contains overall more hydrophobic residues, which are distributed more homogenously all around the helix (Fig. 5G). Strikingly, all residues in the TAP1 TM9 involved in tapasin binding (Asn-411, Ser-412, Thr-414, Thr-415, Gly-419, and Lys-423) are located on the polar face of the amphipathic α-helix (Fig. 5I, *red asterisks*). The respective mutations in construct 1ΔN-YLVRHQ largely introduce hydrophobicity in that area, resulting in the loss of tapasin association (Fig. 5G–I). Importantly, the combined results in Fig. 4 and 5 show that the progressive weakening of the polar character of the TM9 leads to a progressive loss of tapasin binding. Thus, we conclude that the amphipathic transmembrane segment TM9 of the coreTMD of TAP1 binds tapasin via its polar face.

Tapasin binding mutant 1ΔN-YLVRHQ is not a functional TAP1 chain and displays reduced TAP2 association

Because 1ΔN-TM9 had retained significant functional activity (Fig. 3C/D), we expected 1ΔN-YLVRHQ to be a functional TAP1 chain as well. However, when T2 cells pre-expressing this construct were additionally transfected with TAP2 to allow for the formation of assembled TAP heterodimers, no HLA-B,C could be detected at the cell surface (Fig. 6A/B), indicating that 1ΔN-YLVRHQ was non-functional. To show that TAP2 was successfully expressed in these cells, we performed a TAP2-specific RT-PCR, which confirmed that TAP2 mRNA was made (Fig. 6C). Moreover, lysates from two independent clones of T2

cells co-expressing 1ΔN-YLVRHQ and TAP2 clearly contained TAP2 protein (Fig. 6D), and both these clones were surface HLA-B,C-negative (*data not shown*). However, TAP2 levels were reduced when compared to wildtype TAP when normalized to an irrelevant ER protein, Grp94, (Fig. 6D/E, *blue bars*) and the reduction was even more pronounced when normalized to TAP1 (Fig. 6D/E, *black bars*). This is important, because human TAP2 is completely unstable without TAP1 and cannot be detected by Western blot at all if expressed in isolation ((43, 44), and Fig. 6D, *lane 4*). Hence, every TAP2 molecule that can be detected in Western blot is likely a molecule that has been stabilized by TAP1 in an assembled heterodimer. Consistent with this, TAP2 could indeed be co-immunoprecipitated with the 1ΔN-YLVRHQ subunit (Fig. 6F). We therefore conclude that heterodimerization of 1ΔN-YLVRHQ with TAP2 is impaired but not eliminated (Fig. 6D/E). This impairment alone, however, is unlikely to explain the complete absence of surface HLA-B,C expression by T2 cells co-expressing TAP2 and 1ΔN-YLVRHQ, as sufficient levels of heterodimer should exist in the cell to promote at least some surface expression if the mutant transporter were active.

Functional consequences of individual amino acid exchanges in transmembrane segment TM9

To determine which of the six mutations introduced into 1ΔN-YLVRHQ were causing the block in TAP function, we co-expressed a subset of above described mutants, 1ΔN-K423Q*, 1ΔN-R_1Q, 1ΔN-YRHQ, and 1ΔN-YLVRHQ, containing one, two, four, and six mutations in the transmembrane segment, respectively (Fig. 6G), with TAP2, and analyzed whether the respective transporters could promote HLA-B,C surface expression (Fig. 6H). The replacement of Lys-423 with glutamine in construct 1ΔN-K423Q* did not appear to affect TAP function significantly (Fig. 6H). Notably, the related homodimeric peptide transporter TAPL/ABCB9 also contains glutamine in this position. However, the additional exchange of Thr-415 to arginine in construct 1ΔN-R_1Q substantially diminished TAP activity in this assay and the further replacement of Asn-411 and Gly-419 by tyrosine and histidine, respectively, in construct 1ΔN-YRHQ resulted in complete loss of function (Fig. 6H). It is not surprising then that 1ΔN-YLVRHQ, which contains two more mutations (Fig. 6G/7A) was also inactive (Fig. 6H).

To convert these constructs into functional TAP subunits (yet lacking tapasin binding to the coreTMD), we next assessed the functional significance of all four residues affected in loss-of-function construct 1ΔN-YRHQ individually. To this end, we started with construct 1ΔN and mutated Asn-411 to either tyrosine (as in TAP2 and 1ΔN-YRHQ), lysine, or alanine; Thr-415 was mutated to glutamine or alanine; Gly-419 was mutated to histidine (as in TAP2 and 1ΔN-YRHQ) or alanine; Lys-423 was mutated to glutamine (Fig. 7B). After transduction of the respective constructs into a T2 cell clone pre-expressing TAP2 we measured surface HLA-B,C levels by flow cytometry as an indicator of TAP activity. Since the 1ΔN derivatives were linked to EGFP via an IRES site, we gated on EGFP-positive cells in order to analyze only cells that had been successfully transfected (Fig. 7C). As expected, cells only expressing TAP2 alone displayed no TAP activity, whereas construct 1ΔN, if co-expressed with TAP2, promoted high surface HLA-B,C levels (Fig. 7D/E, *white histograms*). Of the four mutations present in the non-functional quadruple mutant 1ΔN-YRHQ, both N411Y and G419H appeared to dramatically reduce TAP function by approximately 75% (Fig. 7E, *red bars*). If it is taken into account that the Thr-415-to-arginine exchange in 1ΔN-YRHQ also diminished the activity of the subunit (Fig. 6H), it is not surprising that this construct is non-functional. Some of the other mutations we introduced into 1ΔN also impaired transporter activity. In particular, N411K and T415Q proved to be problematic, causing a significant and moderate reduction in activity, respectively (Fig. 7E, *red bars*). In contrast, 1ΔN-G419A transfectants had higher HLA-B,C

surface levels than 1ΔN transfectants (Fig. 7E, *red bars*), indicating that Gly419 could be exchanged to alanine without a significant loss of function. Similarly, and consistent with our results in Fig. 6H, the Lys-423-to-glutamine exchange also lead to higher HLA-B,C surface levels (Fig. 7E, *red bars*) suggesting that Lys-423 is not essential for transporter activity, either. Further, the Thr-415-to-alanine mutant, promoted HLA-B,C surface expression to the same extent as the parental construct 1ΔN (Fig. 7E, *red bars*). Mutant N411A was about one third less efficient than 1ΔN in promoting HLA-B,C surface levels, a reduction that may be considered moderate (Fig. 7E, *red bars*).

Mutations in transmembrane segment TM9 can suppress expression problems of 1ΔN

In the experiment shown in Fig. 7C–E we had used a TAP2-expressing clone and transfected it with TAP1 mutants linked to an IRES-EGFP unit. Thus, TAP1 and EGFP should be expressed together on the same mRNA and since we gated on EGFP-positive cells (Fig. 7C), we expected 100% of the analyzed cells to express both the TAP1 mutant and wildtype TAP2. Surprisingly, though, HLA-B,C surface expression was only detected in approximately 25% of the 1ΔN-transfected cells, indicating a high rate of uncoupling of TAP1 expression from the EGFP marker (Fig. 7D, *note the two peaks in white histogram*). This uncoupling was reproducible and always seen when construct 1ΔN was transfected into cells pre-expressing TAP2 (see also Fig. S1A/B, *note the two peaks in white histogram*). However, the phenomenon did not depend on TAP2 expression as EGFP-positive, 1ΔN-negative clones were also obtained when 1ΔN alone was transduced into plain T2 cells (*data not shown*). Interestingly, though, despite the majority of transfectants losing 1ΔN expression after initial introduction of the gene, the population that retained 1ΔN expression stably continued the production of high levels of the mutant indefinitely (*data not shown*). This suggests that although the sudden introduction of 1ΔN may cause problems in the transfected cells, about a quarter of the transfectants are able to adapt to long-term 1ΔN expression eventually. The same uncoupling phenomenon was also observed in all Asn-411 and Thr-415 mutants (Fig. 7D, *note the two peaks in yellow and blue histograms*).

Strikingly, exchanging Gly-419 for histidine or alanine, resulted in all EGFP-positive transfectants expressing the transporter (Fig. 7D, *note only one single peak in green histograms*). Identical observations were made with the mutant in which Lys-423 was exchanged for glutamine and, again, this was reproducible (Fig. 7D, S1A/B, *note only one single peak in the pink histogram*). This may indicate that both Gly-419 and Lys-423 cause problems for the proper insertion of transmembrane segment TM9 in the wildtype molecule and removing those residues relaxes these issues. Consistent with this idea, mutants in which Lys-423 was exchanged for glutamine often displayed higher steady state protein levels than construct 1ΔN (Fig. 4C/G/K, 5B), although expression levels varied from experiment to experiment. Moreover, EGFP fluorescence in the bulk transfectants shown in Fig. 7D was significantly higher for the Gly-419 and Lys-423 mutants than for any other construct (Fig. 7E, *green bars*), further supporting the idea that these mutants were expressed at substantially higher levels.

Construction of a tapasin binding deficient TAP1 mutant predicted to retain functional activity

With the goal of generating a functional version of construct 1ΔN-YRHQ, in which the same residues are mutated but in which the TAP activity was only mildly or not at all affected we generated a quadruple mutant of 1ΔN containing the amino acid exchanges N411A, T415A, G419A, and K423Q, and named it 1ΔN-3AQ (Fig. 7F). We also constructed a potentially improved variant of the non-functional mutant 1ΔN-YLVRHQ, which was based on 1ΔN-3AQ as a parental construct and additionally contained mutations S412A and T414A. This construct was named 1ΔN-5AQ (Fig. 7F). Helical wheel projections show that both

1ΔN-3AQ and 1ΔN-5AQ have lost a charge and contain several hydrophobic amino acids on the formerly polar face of the amphipathic helix TM9 (compare Fig. 7G/H and Fig. 7A). These mutants could be stably expressed in T2 cells (Fig. 7I) and behaved identically to their parental derivatives with respect to tapasin binding. In particular, 1ΔN-3AQ, just as 1ΔN-YRHQ (Fig. 5F), almost completely lost the tapasin interaction, the minimal residual binding requiring long exposure of the respective Western blots to be visualized (Fig. 7J, *lanes 3 and 5*). Further, 1ΔN-5AQ, just as 1ΔN-YLVRHQ (Fig. 5F), displayed no tapasin binding at all (Fig. 7J, *lanes 4 and 6*). Next, we inserted the 3AQ mutation (N411/T415/G419/K423 → A/A/A/Q) (Fig. 7F) into full-length TAP1 (instead of 1ΔN) and expressed this derivative in T2 cells (Fig. 7K). TAP1-3AQ clearly displayed strong tapasin binding, suggesting that the interaction with the coreTMD is not essential to allow the chaperone to interact with the TAP1 N domain (Fig. 7L).

TAP1-3AQ and TAP1-5AQ mutants retain functional activity but display reduced heterodimerization with TAP2

Next, we assessed whether the 3AQ and 5AQ mutations affected TAP1 activity. To this end, we first co-expressed in T2 cells the respective 1ΔN derivatives with TAP2 and examined HLA-B,C surface levels (Fig. 8A/B). In this assay, both 1ΔN-3AQ and 1ΔN-5AQ were functional TAP1 subunits, although 1ΔN-5AQ displayed reduced activity (Fig. 8A/B). Following this, TAP heterodimerization was assessed by Western blotting. Again, human TAP2 alone was undetectable at steady state (Fig. 8C, *lane 2*). Interestingly, 1ΔN stabilized significantly less TAP2 than full-length TAP1 and the same was true for 1ΔN-3AQ and 1ΔN-5AQ (Fig. 8C/D). We note that this was reminiscent of the differential capability of wt-TAP1 and construct 1ΔN-YLVRHQ to stabilize TAP2 (Fig. 6D/E). Moreover, similar observations were also made in radiolabeling experiments (see later in Fig. 9H). We confirmed that different steady state TAP2 protein levels in the respective cell lines were not caused by disparate TAP2 mRNA expression (Fig. 8E). This suggests that the N domain of TAP1 plays an important role in the heterodimerization of the transporter, which raised the question whether the other two tapasin binding sites, the N domain of TAP2 and the transmembrane segment TM9 in TAP1, are also relevant for proper TAP assembly. To test this, we co-expressed in T2 cells TAP2 with full-length wt-TAP1 or TAP1 containing the 3AQ or 5AQ mutations. Additionally, we used a cell line published earlier (25), which co-expressed full-length wt-TAP1 with TAP2 lacking the N domain (2ΔN). All these transporters promoted high levels of surface HLA-B,C and only small, if any, differences to wildtype TAP were observed (Fig. 8F/G). Interestingly, when transporter heterodimerization was assessed in the cell lines, the lack of the N domain in TAP2 seemed to cause a reduction in steady state TAP2 protein levels (Fig. 8H/I, *compare lanes 2 and 5*). Similarly, both TAP1-3AQ and TAP1-5AQ stabilized less TAP2 than wt-TAP (Fig. 8H/I *compare lanes 2, 3, and 4*). Again, all these results were also confirmed in radiolabeling experiments (see later in Fig. 9K) and were not caused by disparate mRNA expression levels in the respective cell lines (Fig. 8J). This indicates that all three regions in TAP, which contain tapasin binding sites (the N domain in TAP1, the N domain in TAP2, and the TM9 in TAP1), are necessary for proper heterodimerization and full stabilization of TAP2. The effect of the coreTMD in TAP1, however, may depend on tapasin binding to the N domain in the same subunit, as constructs 1ΔN-3AQ and 1ΔN-5AQ showed only little, if any, reduction in TAP2 stabilization when compared to construct 1ΔN (Fig. 8C/D).

Tapasin binding mutants are less stable when unassembled and form less stable TAP heterodimers

A major role of tapasin in the MHC class I antigen presentation pathway is the stabilization of TAP (7–9, 27, 28, 42), but it is unknown which tapasin binding site on the transporter subunits is required for this function or whether all are required. To begin to address this

question, we performed pulse-chase experiments in which we analyzed the stability of unassembled mutant or wildtype TAP1 chains stably expressed in T2 cells (Fig. 9A–E). Due to the generally very high stability of both assembled and unassembled TAP1 (45), we chased cells for up to eight hours post labeling. As expected, wt-TAP1 did not noticeably decay at all during this time period (Fig. 9A–E, *black lines*). In contrast, both 1ΔN and TAP1-3AQ, lacking tapasin binding to the N domain and the coreTMD of TAP1, respectively, displayed a slightly diminished stability (Fig. 9C–E, *green and red lines*). However, the effects were rather small and a large number of independent experiments were necessary to show that the difference is statistically significant at the 8h time-point. It seems unlikely that this difference could cause the 3 to >10-fold reduction in TAP1 levels that have been observed in the absence of tapasin (7, 8), let alone the >100-fold reduction in TAP levels that has been observed in tapasin-deficient mouse cells (27). Strikingly, however, constructs simultaneously lacking tapasin binding to both the N domain and the coreTMD (1ΔN-3AQ and 1ΔN-5AQ) dramatically lost stability and presented with half-lives of only four hours (Fig. 9A/B, *green and blue lines*). These results suggest that tapasin binding to both binding sites in TAP1 is necessary to achieve the full stability of unassembled TAP1 chains. Next, we analyzed the effect of the tapasin binding mutations on the stability of assembled TAP heterodimers (Fig. 9F–K). All TAP1 chains lacking the N domain, even 1ΔN, which is fairly stable when unassembled (Fig. 9A/B/C/E, *red lines*), displayed a dramatic loss of stability when co-expressed with TAP2 (Fig. 9F/G, *left panel*, *red line*), perhaps because TAP2 obscures the tapasin binding site in the coreTMD of 1ΔN (18, 23, 24). TAP2 also decayed faster when associated with these TAP1 mutants (Fig. 9F/G, *right panel*), although the accelerated degradation was less pronounced. Strikingly, full-length TAP1 mutants containing the 3AQ or 5AQ mutation were also unstable when co-expressed with TAP2 (Fig. 9I/J, *left panel*) and also conferred less stability on TAP2 (Fig. 9I/J, *right panel*). This suggests that binding of tapasin to the coreTMD of TAP1 may not only be required to generate a normal quantity of TAP heterodimers (Fig. 8H/I and 9I/K), but may also regulate their ultimate stability.

DISCUSSION

MHC class I-mediated antigen presentation is critical for an appropriate immune response against tumors and viruses (1, 2). The pathway depends on the supply of ER-localized MHC class I molecules with peptides, which are mostly of cytosolic origin, the loading of these peptides into the peptide binding groove of MHC class I and their subsequent display at the cell surface to cytotoxic CD8-positive T cells (1, 2). TAP is a key player in this program, mediating the transport of the cytosolic peptides into the ER (4). In the absence of TAP, MHC class I molecules are starved of peptides and as a consequence their surface levels collapse, causing T cells not to recognize their targets anymore (46). Hence, it is not surprising that in order to evade a proper immune response, many tumors down-regulate or even completely eliminate TAP expression (2, 46), while viruses frequently encode specific TAP inhibitors, such as US6, ICP47, or UL49.5 (47).

For a long time it is known that a major function of tapasin in the MHC class I pathway is to stabilize TAP resulting in high steady state protein levels of the transporter (7–9, 27, 28, 42). However, there are three tapasin binding sites in the TAP subunits, one in the N domain of TAP1, one in the N domain of TAP2, and one that was previously identified in the coreTMD of unassembled rat TAP1 ((18). Here we have shown that the latter binding site also exists in human TAP1 (Fig. 1C/D, 2G, 7J/L) and localized it by mutational analysis to the transmembrane segment TM9 (Fig. 2G). The respective roles of these three binding sites in mediating TAP stability are unknown. Furthermore, it is unknown whether tapasin exerts its stabilizing function by acting on the unassembled transporter subunits before heterodimerization or whether it only acts on assembled TAP.

In order to address these questions, we first mapped and characterized the tapasin binding site in the coreTMD of unassembled TAP1. Four amino acid residues in the transmembrane segment TM9 appear to be particularly important: Asn-411, Thr-415, Gly-419, and Lys-423. If these residues are mutated to either the corresponding residues in TAP2 (see construct 1ΔN-YRHQ in Fig. 5C/F and 7J) or to alanine, alanine, alanine, and glutamine, respectively (see construct 1ΔN-3AQ in Fig. 7J), tapasin binding to the coreTMD of TAP1 is almost eliminated. Recently, Corradi and co-workers constructed homology models of the assembled TAP1:TAP2 heterodimer based on published crystal structures from ABC transporters (48). We used two of their models, one based on the inward-facing conformation of ABCB10 (Fig. S2A–C) and one based on the outward-facing conformation of Sav1866 (Fig. S2D–F), in an evaluation of the potential orientation of these critical residues within TM9. Interestingly, in both models none of the four amino acids appear to be accessible from the outside of the assembled transporter. Rather, they point either sideways towards transmembrane helix TM8 or into the pore of the transporter (green residues in Fig. S2A–F). This interpretation of the arrangement is compatible with the fact that the interaction between tapasin and the coreTMD of TAP1 is not observed in the assembled TAP1:TAP2 heterodimer (18, 23, 24). Moreover, it would suggest that in unassembled TAP1 the TM9 segment is rotated outwards within the plane of the membrane so that the key residues become accessible to the docking tapasin molecule.

Much is yet to be learned about interactions between transmembrane helices within lipid bilayers, but a few particular sequence motifs used for such interactions have been identified, including GxxxG (where G stands for glycine and x stands for any amino acid) and its more degenerate cousin SmxxxSm (where Sm stands for a small amino acid, such as glycine, alanine, serine, or threonine) (49). Two of the residues in the transmembrane segment TM9 that we identified as critical for tapasin binding, Thr-415 and Gly-419, participate in such an SmxxxSm motif (TxxxG) (Fig. 2A) and, interestingly, human tapasin may contain a corresponding SmxxxSm motif (GxxxA) spanning residues Gly-405 through Ala-409 (405-GLFKA-409). Besides specific sequence motifs, small polar residues, such as serine, threonine, and asparagine have often been found to contribute to interactions between transmembrane helices (50). Of the four residues mutated in construct TAP1-3AQ, Asn-411 and Thr-415 are polar and both residues that are additionally mutated in construct TAP1-5AQ, Ser-412 and Thr-414, are polar as well (Fig. 7F). Together with Lys-423, all these residues form an extensively polar face in the amphipathic helix TM9 (Fig. 7A). Notably, the stepwise weakening of this polar character causes a progressive loss of tapasin binding, which is completely eliminated in construct 1ΔN-5AQ, in which the polar face has been essentially destroyed (Fig. 4I–L, 5A–F, 7F–J). Thus, consistent with the view that polar residues can make important contributions to interactions between transmembrane helices (49, 50), we propose that the polar face of the TM9 segment mediates the association of unassembled TAP1 with tapasin. We note that although the single transmembrane helix of human tapasin is not exceptionally amphipathic, it does contain a conserved lysine residue at position 408 which lies within above mentioned GxxxA motif, and which has been shown to be critical for TAP stabilization (42).

The transmembrane segment TM9 is not well predicted by topology prediction algorithms (21), probably because of its relatively low hydrophobicity. However, direct topology analysis demonstrated that Thr-399 is located inside the cytosol, while Ser-436 is located inside the ER, showing that the sequence between these two residues, which flank TM9, must span the ER membrane in a cytosol-to-ER orientation (21). Various aspects of our analysis suggest that this segment may cause problems for the membrane integration of TAP1 or at least for the membrane integration of its functional (25) derivative 1ΔN. In particular, a subset of T2 cells forced to produce 1ΔN (and many of its derivatives) by transduction appears to have a strong tendency to lose expression of the construct even

though they retain EGFP, expressed from the same mRNA via an IRES site (Fig. 7C/D, S1A/B). The mechanism behind this uncoupling and why it occurs only in some but not in all cells (see the Results section) is unclear. Strikingly, this problem can be completely eliminated by mutation of the transmembrane segment TM9. One way to fully suppress the TAP1/EGFP uncoupling is to replace the charged Lys-423 with glutamine (Fig. 7C/D, S1A/B), the corresponding residue in TAP2 and in the TAP-related peptide ABC transporter TAPL/ABCB9. This not only reproducibly abrogates the loss of 1ΔN by a subset of cells, but also appears to allow overall higher expression of the mRNA as both EGFP levels (Fig. 7E, S1A) and 1ΔN protein levels are increased (Fig. 4G).

The problem of 1ΔN expression is also resolved by the exchange of Gly-419 with either alanine or histidine (Fig. 7C–E). While it may be obvious that a charged amino acid such as Lys-423 might be problematic in a transmembrane segment, it is less clear why glycine would cause such difficulties. Although regarded as a classical “helix breaker” in soluble proteins, glycine is a very common amino acid in transmembrane helices, and the hydrophobic environment within the membrane bilayer typically favors its incorporation into such segments (50). Nevertheless, constraining the glycine backbone by tethering it into a helical structure has an entropic cost (50) and may make Gly-419 in its particular environment a suboptimal amino acid in that position. Given that both Lys-423 and Gly-419 appear to be involved in tapasin binding it is possible that it is not the nature of the TM segment as such but the tapasin interaction with the coreTMD that is ultimately causing the expression problems of 1ΔN. However, arguing against this, the 1ΔN-K423Q mutant largely retains tapasin binding activity (Fig. 4H) and even mutant 1ΔN-RHQ, in which both Gly-419 and Lys-423 are mutated, still displays a low level of tapasin association (Fig. 4L, 5C). Nevertheless, we cannot exclude the possibility that tapasin binds to these mutants in a subtly modified manner compared to the parental 1ΔN construct.

Nothing is known so far about a possible function that tapasin binding to the coreTMD of unassembled TAP1 may serve. Thus, the mutants generated in this study could also provide some functional insights into this interaction. To this end, we had constructed all our mutants as domain-swapping or point mutants rather than deletion mutants in order to produce potentially functional transporter subunits whose activity and thus overall proper folding can be confirmed in assays such as flow cytometry analysis of HLA-B,C cell surface levels (Fig. 8A/B/F/G). Interestingly, TAP1 lacking the tapasin interaction with the coreTMD appears to be less efficient in forming a dimer with TAP2 (Fig. 8H–J, 9K) and a similar defect was observed with both TAP1 and TAP2 N domain deletion mutants (Fig. 8C–E, Fig. 8H–J, 9H/K). Consistent with this, the association of rat-derived 1ΔN and 2ΔN was previously shown to be strongly diminished *in vitro* compared to the intact subunits (51). This suggests that all three tapasin binding sites in the TAP subunits may cooperate to achieve maximally efficient dimer formation.

Interestingly, the absence of the tapasin binding site in the coreTMD only appears to have a significant negative effect on heterodimerization if tapasin binding to the N domain of TAP1 is intact, *i.e*. introducing the 3AQ or 5AQ mutation affects the heterodimerization of full-length TAP1 (Fig. 8H–J, 9K) but does not further impede dimer assembly when introduced into 1ΔN (Fig. 8C–E, 9H). One possible explanation for this could be that the two tapasin binding sites in unassembled TAP1 cooperate in tethering and orienting a shared tapasin molecule in a manner that allows efficient association with an incoming TAP2 molecule. In such a model, disturbing either tapasin docking site could be sufficient to altogether lose the assistance the chaperone normally provides to the process. In order to form a complete TAP dimer, TAP1 must be made first and subsequently associate with a newly synthesized, nascent TAP2 chain (45). TAP2 entering the complex, however, would have to displace tapasin from the coreTMD as assembled TAP cannot sustain this interaction (18). The

chaperone would either be fully released from the nascent transporter, captured by the N domain of TAP1 or it may even be picked up by the N domain of TAP2. How could deficient tapasin binding impair the TAP1:TAP2 dimerization process? One plausible way would be by causing a lower rate of TAP dimer initiation (*i.e*. causing a lower rate of capturing TAP2 into the complex). Once fully synthesized, unassembled TAP2 loses its ability to form a dimer with TAP1 and is unstable and rapidly degraded (45). However, it remains possible that proper tapasin association is required to organize molecules within a rearranging TAP complex and lack of this association may lead to subtly altered transporter dimers which are less stable.

The capacity of tapasin to stabilize TAP is well established (7–9, 27, 28, 42), so it was not surprising to find that the decay rate of the TAP1 subunit depends on tapasin binding (Fig. 9A–E). However, earlier reports noted that unassembled rat-derived 1ΔN was surprisingly stable, raising speculations that it might be the binding of tapasin to the coreTMD that is key to stabilize TAP1 (18). We therefore compared in a purely human experimental system the stability of 1ΔN and TAP1-3AQ, lacking tapasin binding to one or the other binding site. Surprisingly, both constructs, when unassembled, were fairly stable, showing only a slightly faster decay than the wildtype subunit (Fig. 9C–E). This suggests that tapasin binding to either of the two docking sites is sufficient to significantly stabilize the protein. Strikingly, though, when binding to both sites was abolished as in constructs 1ΔN-3AQ and 1ΔN-5AQ, a drastic loss of stability was observed resulting in half-lives of only approximately 4h (Fig. 9A/B). These results suggest that both tapasin binding sites in TAP1 may be functionally redundant to some extent with respect to stabilizing TAP but that both sites cooperate to achieve the full stability of the molecule.

In summary, our results demonstrate that human unassembled TAP1 interacts with tapasin via the coreTMD. We map this interaction to transmembrane segment TM9 and find that within the respective amphipathic helix it is the polar face that drives the association. Within this polar face, we identify critical amino acid residues necessary for tapasin binding. Experiments using mutant TAP1 subunits that are deficient in tapasin binding to the coreTMD suggest that this interaction plays a role in both heterodimerization and stabilization of the transporter. Thus, our results provide novel insights into the network of interactions that guide the assembly and biogenesis of TAP and the peptide loading complex, a process critical for MHC class I-mediated immunity.

Supplementary Material

Refer to Web version on PubMed Central for supplementary material.

Acknowledgments

We are indebted to Dr. J. McCluskey for his kind donation of the tapasin-specific monoclonal antibody 3H6 and thank J. Cresswell for technical assistance. Drs. C. Paduraru, J. Grotzke, and D. Sengupta are acknowledged for critically reading the manuscript.

This study was supported by the Howard Hughes Medical Institute, Yale SPORE in Skin Cancer Grant *5P50 CA121974*, and NIH Grants *R37-AI023081* and *R01-AI097206* (to PC), a Cancer Research Institute Fellowship (to RML), and an MSTP Fellowship (*NIH MSTP TG T32GM07205*) (to PA).

ABBREVIATIONS LIST

ABC	ATP-binding cassette
ER	endoplasmic reticulum

FCS	fetal calf serum
MHC	major histocompatibility complex
NBD	nucleotide binding domain
N domains	N-terminal domains
PLC	peptide loading complex
TAP	transporter associated with antigen processing
TM	transmembrane
TMD	transmembrane domain
coreTMD	core transmembrane domain

REFERENCES

1. Van Kaer L. Major histocompatibility complex class I-restricted antigen processing and presentation. Tissue antigens. 2002; 60:1–9. [PubMed: 12366777]
2. Dimberu PM, Leonhardt RM. Cancer immunotherapy takes a multi-faceted approach to kick the immune system into gear. The Yale journal of biology and medicine. 2011; 84:371–380. [PubMed: 22180675]
3. Vigneron N, Van den Eynde BJ. Proteasome subtypes and the processing of tumor antigens: increasing antigenic diversity. Current opinion in immunology. 2012; 24:84–91. [PubMed: 22206698]
4. Procko E, Gaudet R. Antigen processing and presentation: TAPping into ABC transporters. Current opinion in immunology. 2009; 21:84–91. [PubMed: 19261456]
5. Sadasivan B, Lehner PJ, Ortmann B, Spies T, Cresswell P. Roles for calreticulin and a novel glycoprotein, tapasin, in the interaction of MHC class I molecules with TAP. Immunity. 1996; 5:103–114. [PubMed: 8769474]
6. Koch J, Guntrum R, Tampe R. The first N-terminal transmembrane helix of each subunit of the antigenic peptide transporter TAP is essential for independent tapasin binding. FEBS letters. 2006; 580:4091–4096. [PubMed: 16828748]
7. Lehner PJ, Surman MJ, Cresswell P. Soluble tapasin restores MHC class I expression and function in the tapasin-negative cell line .220. Immunity. 1998; 8:221–231. [PubMed: 9492003]
8. Tan P, Kropshofer H, Mandelboim O, Bulbuc N, Hammerling GJ, Momburg F. Recruitment of MHC class I molecules by tapasin into the transporter associated with antigen processing-associated complex is essential for optimal peptide loading. J Immunol. 2002; 168:1950–1960. [PubMed: 11823531]
9. Bangia N, Lehner PJ, Hughes EA, Surman M, Cresswell P. The N-terminal region of tapasin is required to stabilize the MHC class I loading complex. European journal of immunology. 1999; 29:1858–1870. [PubMed: 10382748]
10. Chen M, Bouvier M. Analysis of interactions in a tapasin/class I complex provides a mechanism for peptide selection. The EMBO journal. 2007; 26:1681–1690. [PubMed: 17332746]
11. Howarth M, Williams A, Tolstrup AB, Elliott T. Tapasin enhances MHC class I peptide presentation according to peptide half-life. Proceedings of the National Academy of Sciences of the United States of America. 2004; 101:11737–11742. [PubMed: 15286279]
12. Stroobant V, Demotte N, Luiten RM, Leonhardt RM, Cresswell P, Bonehill A, Michaux A, Ma W, Mulder A, Van den Eynde BJ, van der Bruggen P, Vigneron N. Inefficient exogenous loading of a tapasin-dependent peptide onto HLA-B*44:02 can be improved by acid treatment or fixation of target cells. European journal of immunology. 2012; 42:1417–1428. [PubMed: 22678898]
13. Vigneron N, Peaper DR, Leonhardt RM, Cresswell P. Functional significance of tapasin membrane association and disulfide linkage to ERp57 in MHC class I presentation. European journal of immunology. 2009; 39:2371–2376. [PubMed: 19701894]

14. Wearsch PA, Cresswell P. Selective loading of high-affinity peptides onto major histocompatibility complex class I molecules by the tapasin-ERp57 heterodimer. Nat Immunol. 2007; 8:873–881. [PubMed: 17603487]
15. Williams AP, Peh CA, Purcell AW, McCluskey J, Elliott T. Optimization of the MHC class I peptide cargo is dependent on tapasin. Immunity. 2002; 16:509–520. [PubMed: 11970875]
16. Howe C, Garstka M, Al-Balushi M, Ghanem E, Antoniou AN, Fritzsche S, Jankevicius G, Kontouli N, Schneeweiss C, Williams A, Elliott T, Springer S. Calreticulin-dependent recycling in the early secretory pathway mediates optimal peptide loading of MHC class I molecules. The EMBO journal. 2009; 28:3730–3744. [PubMed: 19851281]
17. Leonhardt RM, Fiegl D, Rufer E, Karger A, Bettin B, Knittler MR. Post-endoplasmic reticulum rescue of unstable MHC class I requires proprotein convertase PC7. J Immunol. 2010; 184:2985–2998. [PubMed: 20164418]
18. Leonhardt RM, Keusekotten K, Bekpen C, Knittler MR. Critical role for the tapasin-docking site of TAP2 in the functional integrity of the MHC class I-peptide-loading complex. J Immunol. 2005; 175:5104–5114. [PubMed: 16210614]
19. Zhang W, Wearsch PA, Zhu Y, Leonhardt RM, Cresswell P. A role for UDP-glucose glycoprotein glucosyltransferase in expression and quality control of MHC class I molecules. Proceedings of the National Academy of Sciences of the United States of America. 2011; 108:4956–4961. [PubMed: 21383159]
20. Ehses S, Leonhardt RM, Hansen G, Knittler MR. Functional role of C-terminal sequence elements in the transporter associated with antigen processing. J Immunol. 2005; 174:328–339. [PubMed: 15611256]
21. Schrodt S, Koch J, Tampe R. Membrane topology of the transporter associated with antigen processing (TAP1) within an assembled functional peptide-loading complex. The Journal of biological chemistry. 2006; 281:6455–6462. [PubMed: 16407277]
22. Hulpke S, Tomioka M, Kremmer E, Ueda K, Abele R, Tampe R. Direct evidence that the N-terminal extensions of the TAP complex act as autonomous interaction scaffolds for the assembly of the MHC I peptide-loading complex. Cell Mol Life Sci. 2012; 69:3317–3327. [PubMed: 22638925]
23. Koch J, Guntrum R, Heintke S, Kyritsis C, Tampe R. Functional dissection of the transmembrane domains of the transporter associated with antigen processing (TAP). The Journal of biological chemistry. 2004; 279:10142–10147. [PubMed: 14679198]
24. Procko E, Raghuraman G, Wiley DC, Raghavan M, Gaudet R. Identification of domain boundaries within the N-termini of TAP1 and TAP2 and their importance in tapasin binding and tapasin-mediated increase in peptide loading of MHC class I. Immunology and cell biology. 2005; 83:475–482. [PubMed: 16174096]
25. Panter MS, Jain A, Leonhardt RM, Ha T, Cresswell P. Dynamics of major histocompatibility complex class I association with the human peptide-loading complex. The Journal of biological chemistry. 2012; 287:31172–31184. [PubMed: 22829594]
26. Rufer E, Leonhardt RM, Knittler MR. Molecular architecture of the TAP-associated MHC class I peptide-loading complex. J Immunol. 2007; 179:5717–5727. [PubMed: 17947644]
27. Garbi N, Tiwari N, Momburg F, Hammerling GJ. A major role for tapasin as a stabilizer of the TAP peptide transporter and consequences for MHC class I expression. European journal of immunology. 2003; 33:264–273. [PubMed: 12594855]
28. Papadopoulos M, Momburg F. Multiple residues in the transmembrane helix and connecting peptide of mouse tapasin stabilize the transporter associated with the antigen-processing TAP2 subunit. The Journal of biological chemistry. 2007; 282:9401–9410. [PubMed: 17244610]
29. Salter RD, Howell DN, Cresswell P. Genes regulating HLA class I antigen expression in T-B lymphoblast hybrids. Immunogenetics. 1985; 21:235–246. [PubMed: 3872841]
30. Peaper DR, Cresswell P. The redox activity of ERp57 is not essential for its functions in MHC class I peptide loading. Proceedings of the National Academy of Sciences of the United States of America. 2008; 105:10477–10482. [PubMed: 18650385]
31. Ortmann B, Androlewicz MJ, Cresswell P. MHC class I/beta 2-microglobulin complexes associate with TAP transporters before peptide binding. Nature. 1994; 368:864–867. [PubMed: 8159247]

32. Meyer TH, van Endert PM, Uebel S, Ehring B, Tampe R. Functional expression and purification of the ABC transporter complex associated with antigen processing (TAP) in insect cells. FEBS letters. 1994; 351:443–447. [PubMed: 8082812]
33. Dick TP, Bangia N, Peaper DR, Cresswell P. Disulfide bond isomerization and the assembly of MHC class I-peptide complexes. Immunity. 2002; 16:87–98. [PubMed: 11825568]
34. Stam NJ, Spits H, Ploegh HL. Monoclonal antibodies raised against denatured HLA-B locus heavy chains permit biochemical characterization of certain HLA-C locus products. J Immunol. 1986; 137:2299–2306. [PubMed: 3760563]
35. Trapani JA, Mizuno S, Kang SH, Yang SY, Dupont B. Molecular mapping of a new public HLA class I epitope shared by all HLA-B and HLA-C antigens and defined by a monoclonal antibody. Immunogenetics. 1989; 29:25–32. [PubMed: 2461903]
36. van Endert PM, Tampe R, Meyer TH, Tisch R, Bach JF, McDevitt HO. A sequential model for peptide binding and transport by the transporters associated with antigen processing. Immunity. 1994; 1:491–500. [PubMed: 7895159]
37. Barton GM, Medzhitov R. Retroviral delivery of small interfering RNA into primary cells. Proceedings of the National Academy of Sciences of the United States of America. 2002; 99:14943–14945. [PubMed: 12417750]
38. Leonhardt RM, Vigneron N, Hee JS, Graham M, Cresswell P. Critical residues in the PMEL/Pmel17 N-terminus direct the hierarchical assembly of melanosomal fibrils. Molecular biology of the cell. 2013; 24:964–981. [PubMed: 23389629]
39. Leonhardt RM, Lee SJ, Kavathas PB, Cresswell P. Severe tryptophan starvation blocks onset of conventional persistence and reduces reactivation of Chlamydia trachomatis. Infect Immun. 2007; 75:5105–5117. [PubMed: 17724071]
40. Leonhardt RM, Vigneron N, Rahner C, Van den Eynde BJ, Cresswell P. Endoplasmic reticulum export, subcellular distribution, and fibril formation by Pmel17 require an intact N-terminal domain junction. The Journal of biological chemistry. 2010; 285:16166–16183. [PubMed: 20231267]
41. Leonhardt RM, Vigneron N, Rahner C, Cresswell P. Proprotein convertases process Pmel17 during secretion. The Journal of biological chemistry. 2011; 286:9321–9337. [PubMed: 21247888]
42. Petersen JL, Hickman-Miller HD, McIlhaney MM, Vargas SE, Purcell AW, Hildebrand WH, Solheim JC. A charged amino acid residue in the transmembrane/cytoplasmic region of tapasin influences MHC class I assembly and maturation. J Immunol. 2005; 174:962–969. [PubMed: 15634919]
43. Furukawa H, Murata S, Yabe T, Shimbara N, Keicho N, Kashiwase K, Watanabe K, Ishikawa Y, Akaza T, Tadokoro K, Tohma S, Inoue T, Tokunaga K, Yamamoto K, Tanaka K, Juji T. Splice acceptor site mutation of the transporter associated with antigen processing-1 gene in human bare lymphocyte syndrome. The Journal of clinical investigation. 1999; 103:755–758. [PubMed: 10074494]
44. Seliger B, Ritz U, Abele R, Bock M, Tampe R, Sutter G, Drexler I, Huber C, Ferrone S. Immune escape of melanoma: first evidence of structural alterations in two distinct components of the MHC class I antigen processing pathway. Cancer research. 2001; 61:8647–8650. [PubMed: 11751378]
45. Keusekotten K, Leonhardt RM, Ehses S, Knittler MR. Biogenesis of functional antigenic peptide transporter TAP requires assembly of pre-existing TAP1 with newly synthesized TAP2. The Journal of biological chemistry. 2006; 281:17545–17551. [PubMed: 16624807]
46. Seliger B, Maeurer MJ, Ferrone S. TAP off--tumors on. Immunology today. 1997; 18:292–299. [PubMed: 9190116]
47. Ressing ME, Luteijn RD, Horst D, Wiertz EJ. Viral interference with antigen presentation: trapping TAP. Molecular immunology. 2013; 55:139–142. [PubMed: 23141382]
48. Corradi V, Singh G, Tieleman DP. The human transporter associated with antigen processing: molecular models to describe peptide binding competent states. The Journal of biological chemistry. 2012; 287:28099–28111. [PubMed: 22700967]
49. Li E, Wimley WC, Hristova K. Transmembrane helix dimerization: beyond the search for sequence motifs. Biochimica et biophysica acta. 2012; 1818:183–193. [PubMed: 21910966]

50. Javadpour MM, Eilers M, Groesbeek M, Smith SO. Helix packing in polytopic membrane proteins: role of glycine in transmembrane helix association. Biophysical journal. 1999; 77:1609–1618. [PubMed: 10465772]

51. Leonhardt, RM. Doctoral dissertation. Cologne: University of Cologne; 2005. Molecular and functional characterization of early and late checkpoints in the quality control of MHC class I-restricted antigen presentation.

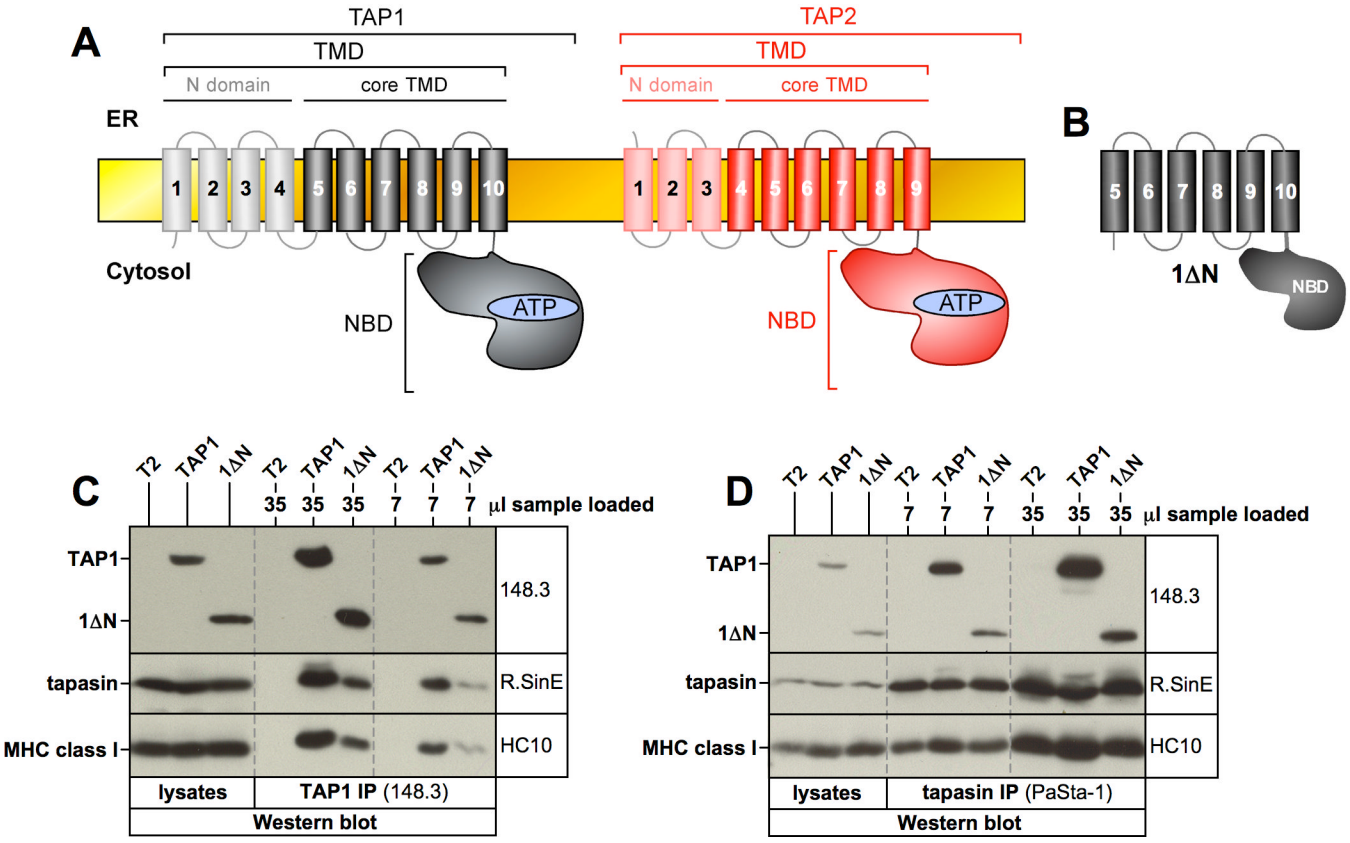

Figure 1. The core transmembrane domain (coreTMD) of human TAP1 contains a tapasin binding site

A) Schematic representation and domain organization of the TAP subunits TAP1 (*black*) and TAP2 (*red*). **B)** Schematic representation of the 1ΔN construct lacking the N domain. **C, D)** TAP1 (C) or tapasin (D) were immunoprecipitated with the indicated antibodies from digitonin lysates of untransfected T2 cells or stable T2 transfectants expressing full-length wildtype TAP1 or construct 1ΔN. Isolated proteins were analyzed by Western blotting using antibodies against TAP (148.3), tapasin (R.SinE), and MHC class I (HC10). Vertical dashed lines indicate positions where irrelevant lanes have been removed from the image.

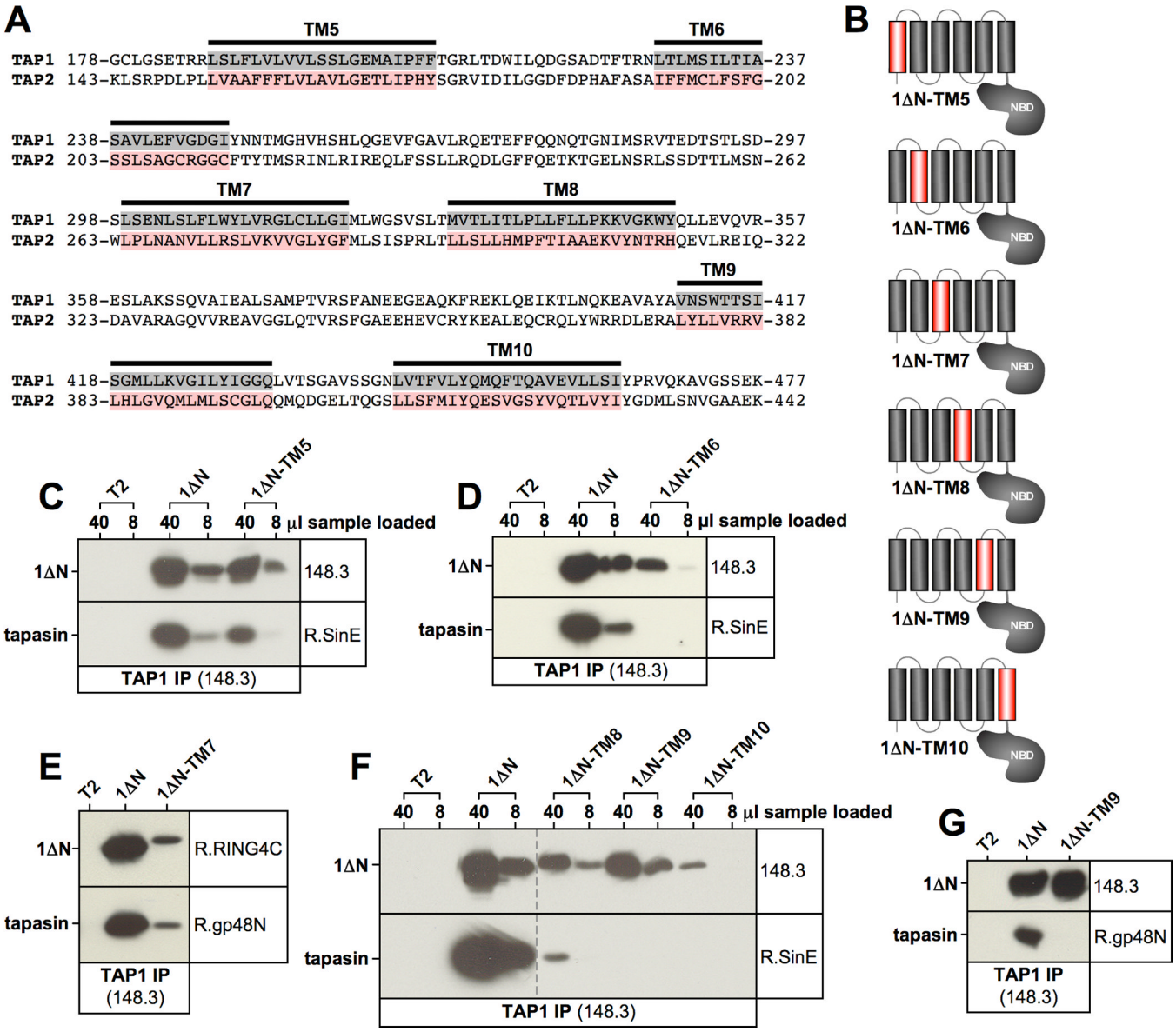

Figure 2. The TAP1 transmembrane segment TM9 contains a tapasin binding site

A) Collinear alignment of part of the coreTMDs of TAP1 and TAP2. The six transmembrane segments in the coreTMD of TAP1 are highlighted in grey (TM5 through TM10). The corresponding sequences in TAP2 to which these were exchanged in constructs 1ΔN-TM5 through 1ΔN-TM10 are shown in red. **B)** Schematic representation of the TAP1-TAP2 hybrid mutants of construct 1ΔN, in each of which one transmembrane segment was replaced by the corresponding sequence in TAP2 (*red*). **C–G)** TAP1 was immunoprecipitated with antibody 148.3 from digitonin lysates of untransfected T2 cells or the indicated stable T2 transfectants. Because construct 1ΔN-TM6 could be only very poorly expressed, we immunoprecipitated from a significantly larger number of cells (8×10^7 cells instead of 1×10^7 cells) in the experiment shown in Fig. 2D. Isolated proteins were analyzed by Western blotting using antibodies against TAP1 (148.3 or R.RING4C) and tapasin (R.SinE or R.gp48N). Vertical dashed lines indicate positions where irrelevant lanes have been removed from the image.

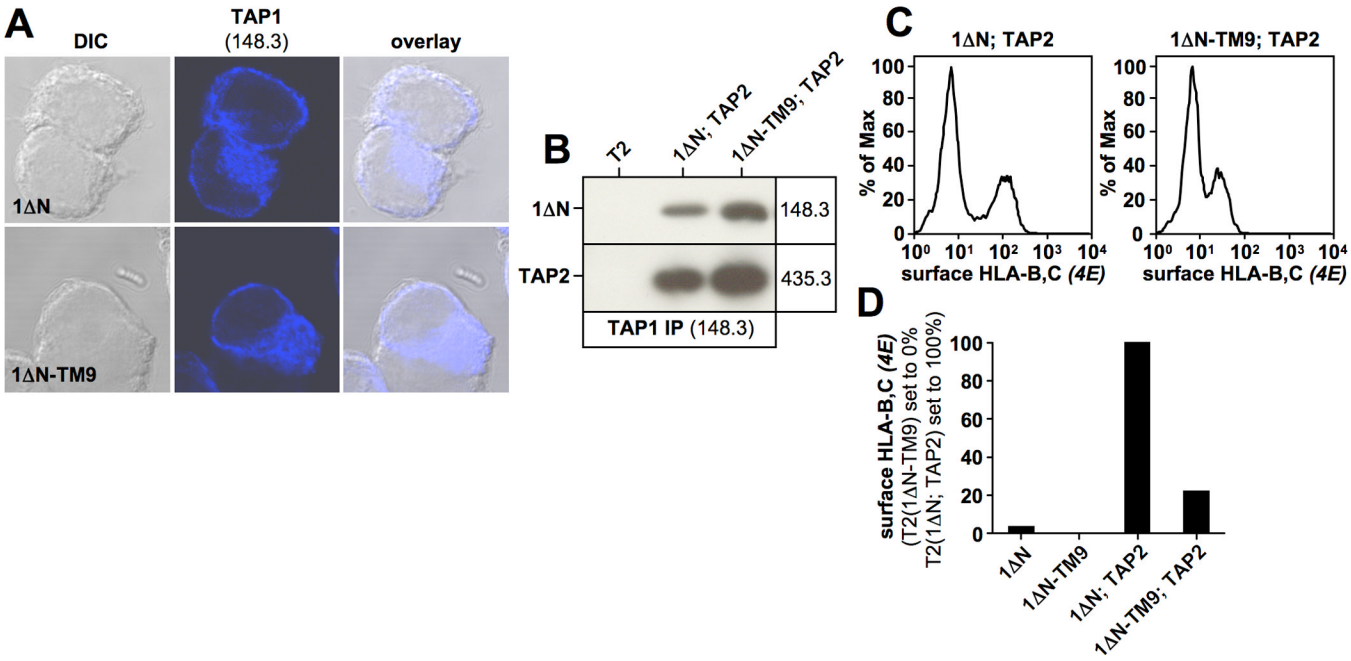

Figure 3. 1ΔN-TM9 localizes to the endoplasmic reticulum and retains function to a significant extent

A) Immunofluorescence analysis of the indicated T2 transfectants using the TAP1-specific antibody 148.3. **B)** TAP1 was immunoprecipitated with antibody 148.3 from a digitonin lysate of the stable T2 transfectant expressing 1ΔN-TM9. Isolated proteins were analyzed by Western blotting using antibodies against TAP1 (148.3) and TAP2 (435.3). **C, D)** Flow cytometry analysis of surface-HLA-B,C expression using antibody 4E in the indicated T2 transfectants (C). Surface-HLA-B,C levels are shown as a bar diagram (1ΔN; TAP2 set to 100%) (D).

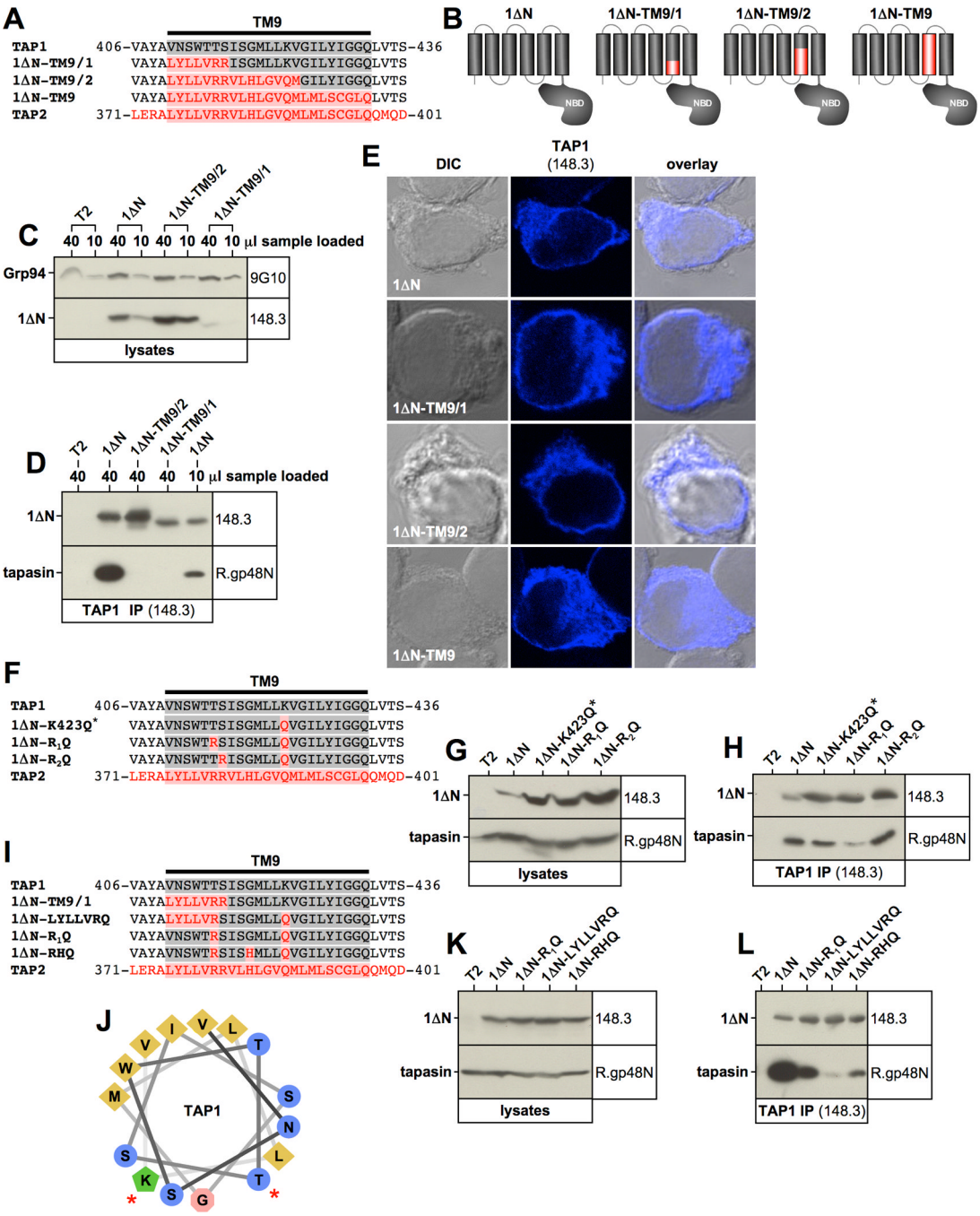

Figure 4. The N-terminal third of transmembrane segment TM9 plays an important role in tapasin interaction

A, F, I) Alignment of the TAP1-TM9, the corresponding TAP2 sequence, and selected mutants. TAP1 sequences are shown in grey. TAP2 sequences are shown in red. **B)** Schematic representation of 1ΔN mutant constructs. **C, G, K)** Western blot analysis showing digitonin lysates from stable T2 transfectants using antibodies recognizing TAP1 (148.3), Grp94 (9G10), and tapasin (R.gp48N). **D, H, L)** TAP1 was immunoprecipitated with antibody 148.3 from digitonin lysates of untransfected T2 cells or the indicated stable T2 transfectants. Isolated proteins were analyzed by Western blotting using antibodies against TAP1 (148.3) and tapasin (R.gp48N). **E)** Immunofluorescence analysis of the indicated T2

transfectants using the TAP1-specific antibody 148.3. **J)** Helical wheel projection of the first two thirds of the TAP1 transmembrane segment TM9. Residues whose mutation result in reduced tapasin binding are indicated with a red asterisk.

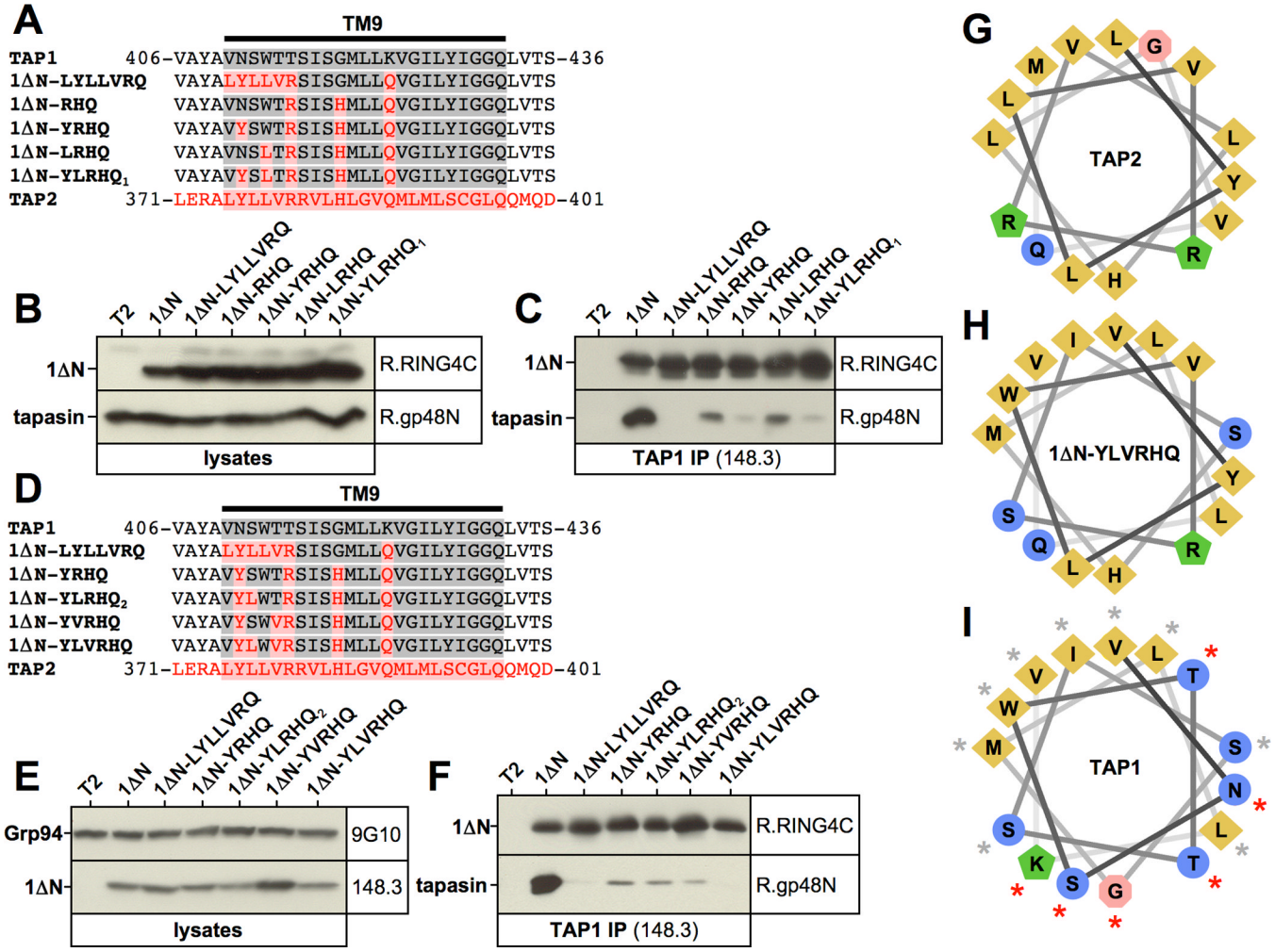

Figure 5. Identification of key amino acid residues within TAP1 transmembrane segment TM9 that are involved in tapasin binding

A, D) Alignment of the TAP1-TM9, the corresponding TAP2 sequence, and selected mutants. TAP1 sequences are shown in grey. TAP2 sequences are shown in red. **B, E)** Western blot analysis showing digitonin lysates from stable T2 transfectants using antibodies recognizing TAP1 (148.3 or R.RING4C), Grp94 (9G10), and tapasin (R.gp48N). **C, F)** TAP1 was immunoprecipitated with antibody 148.3 from digitonin lysates of untransfected T2 cells or the indicated stable T2 transfectants. Isolated proteins were analyzed by Western blotting using antibodies against TAP1 (R.RING4C) and tapasin (R.gp48N). **G, H, I)** Helical wheel projection of the first two thirds of the TAP1 transmembrane segment TM9 (I) or the corresponding sequences from 1ΔN-YLVRHQ (H) or TAP2 (G). Residues in TAP1 whose mutation result in reduced tapasin binding are indicated with a red asterisk in (I).

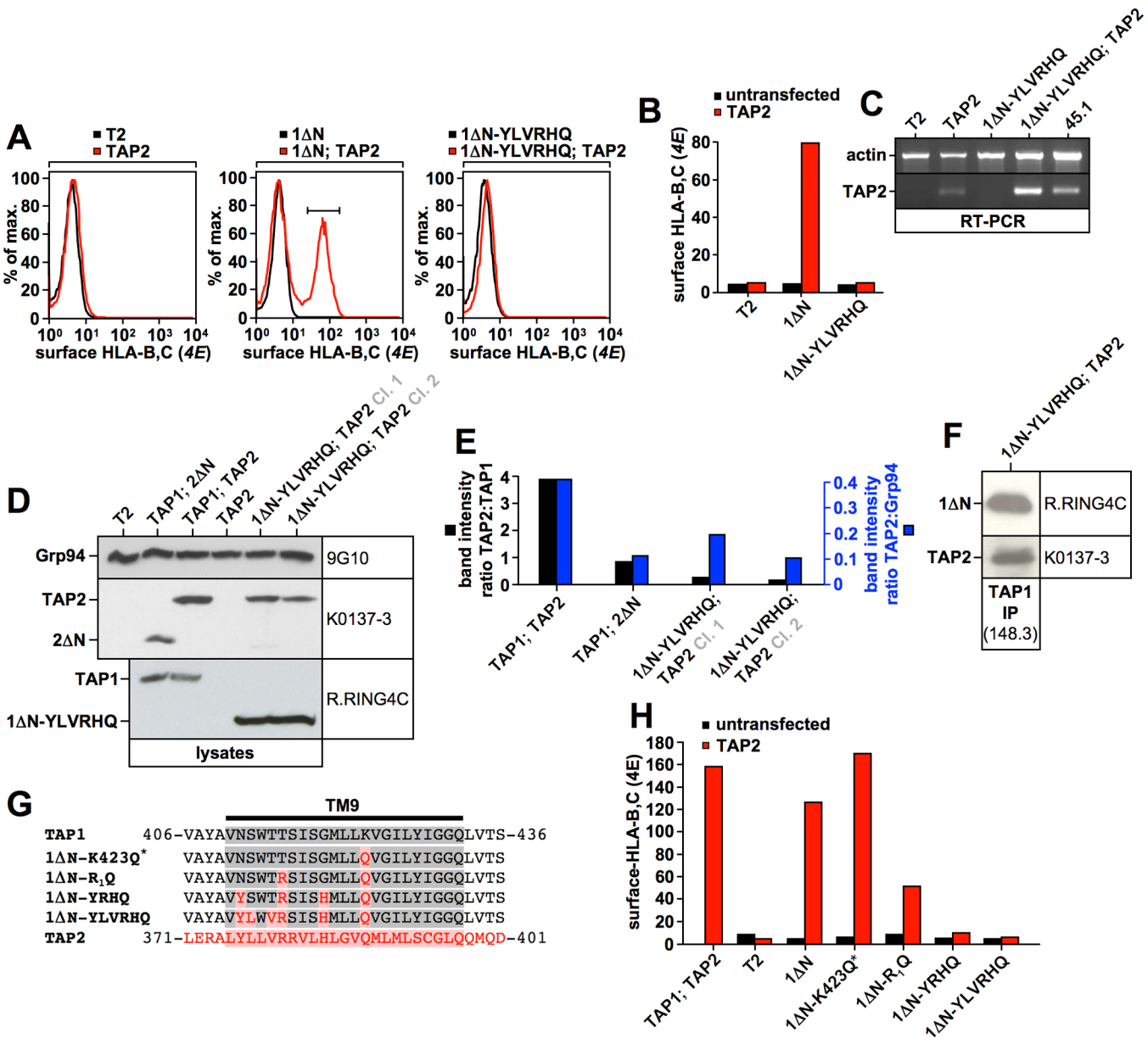

Figure 6. Constructs 1ΔN-YRHQ and 1ΔN-YLVRHQ are non-functional

A, B) Flow cytometry analysis of surface-HLA-B,C expression using antibody 4E in the indicated T2 transfectants (A). Black histograms correspond to untransfected T2 cells or T2 cells expressing TAP1 mutants alone. Red histograms correspond to T2 cells expressing TAP2 or co-expressing TAP2 and a TAP1 mutant. Surface-HLA-B,C levels are shown as a bar diagram (color code as in Fig. 6A) (B). **C)** RT-PCR using actin- or TAP2-specific primers. **D, E)** Western blot analysis showing digitonin lysates from stable T2 transfectants using antibodies recognizing TAP1 (R.RING4C), Grp94 (9G10), and TAP2 (K0137-3). The bar diagram in Fig. 6E displays the quantification of the Western blot in Fig. 6D. TAP2 levels normalized to TAP1 are shown in black. TAP2 levels normalized to Grp94 are shown in blue. **F)** TAP1 was immunoprecipitated with antibody 148.3 from digitonin lysates of T2 cells stably co-expressing 1ΔN-YLVRHQ and TAP2. Isolated proteins were analyzed by Western blotting using antibodies against TAP1 (R.RING4C) and TAP2 (K0137-3). **G)** Alignment of the TAP1-TM9, the corresponding TAP2 sequence, and selected mutants.

TAP1 sequences are shown in grey. TAP2 sequences are shown in red. **H)** Flow cytometry analysis of surface-HLA-B,C expression using antibody 4E in the indicated T2 transfectants (color code as in Fig. 6A/B). Surface-HLA-B,C levels are shown as a bar diagram.

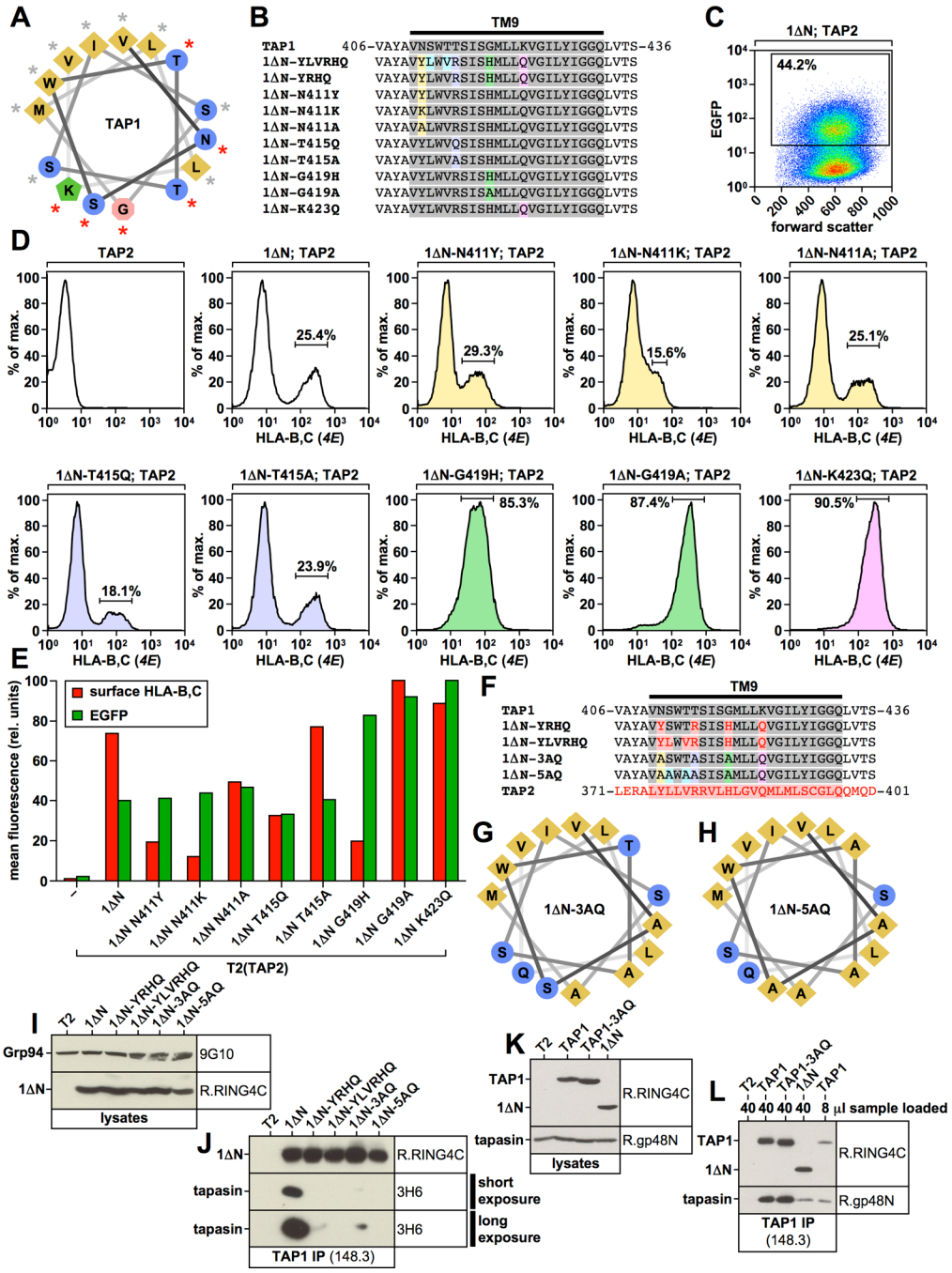

Figure 7. Functional analysis of 1ΔN point mutants

A) Helical wheel projection of the first two thirds of the TAP1 transmembrane segment TM9. Residues whose mutation result in reduced tapasin binding are indicated with a red asterisk. **B)** Alignment of the TAP1-TM9 and selected point mutants. TAP1 sequences are shown in grey. Point mutations are highlighted in color. **C)** Flow cytometry analysis showing EGFP expression versus forward scatter for the T2 transfectant co-expressing 1ΔN and TAP2. The EGFP-positive population is shown in the gate. **D, E)** Flow cytometry analysis of surface-HLA-B,C expression using antibody 4E in the indicated T2 transfectants. Results were first gated on living cells (propidium iodide-negative), then on EGFP-positive

cells using the gate shown in Fig. 7C. Cells expressing TAP2 alone (*first histogram in upper row*) were not gated on EGFP. The color code of the histograms corresponds to the color code used in Fig. 7B. The flow cytometry results are shown as a bar diagram in Fig. 7E (*red bars, surface-HLA-B,C levels*; *green bars, EGFP fluorescence*). **F)** Alignment of the TAP1-TM9, the corresponding TAP2 sequence, and selected mutants. TAP1 sequences are shown in grey. TAP2 sequences are shown in red. The color code for mutations in constructs 1ΔN-3AQ and 1ΔN-5AQ is adapted from Fig. 7B/D. **G, H)** Helical wheel projection of the first two thirds of the transmembrane segment TM9 in mutants 1ΔN-3AQ and 1ΔN-5AQ. **I, K)** Western blot analysis showing digitonin lysates from stable T2 transfectants using antibodies recognizing TAP1 (R.RING4C), Grp94 (9G10), or tapasin (R.gp48N). **J, L)** TAP1 was immunoprecipitated with antibody 148.3 from digitonin lysates of untransfected T2 cells or the indicated stable T2 transfectants. Isolated proteins were analyzed by Western blotting using antibodies against TAP1 (R.RING4C) and tapasin (R.gp48N or 3H6).

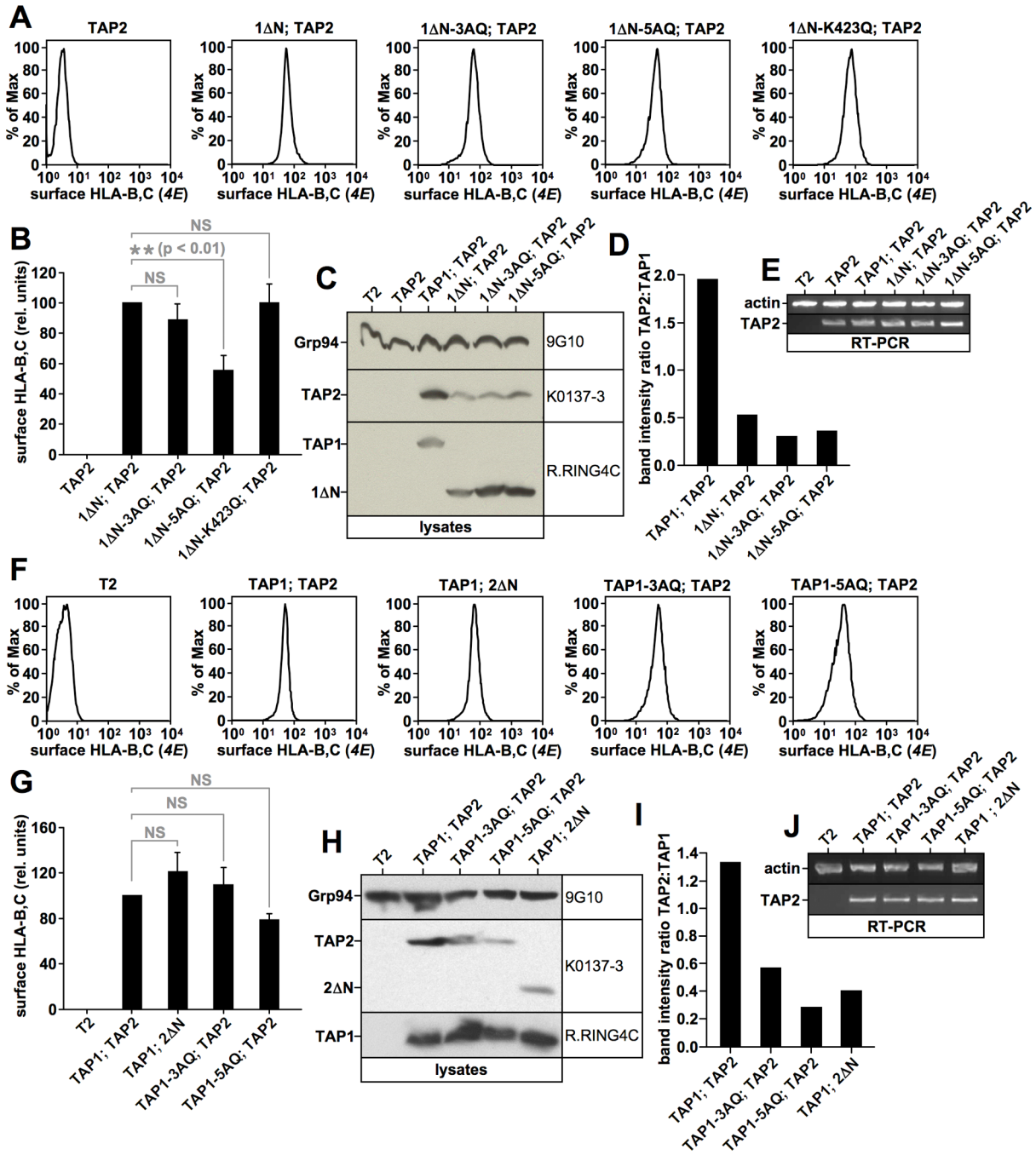

Figure 8. Tapasin binding mutants of TAP retain peptide transport activity but display impaired heterodimerization

A, B) Flow cytometry analysis of surface-HLA-B,C expression using antibody 4E in the indicated T2 transfectants. Results were gated on living, propidium iodide-negative cells (A). Flow cytometry results showing the averages of four independent experiments including the one depicted in Fig. 8A are shown as a bar diagram (B). The error bars are showing the standard deviation from the mean. Statistical analysis was performed by a repeated measures ANOVA test followed by Dunnett's post-test using Prism 4.0 (GraphPad Software) (NS, not significant). **C, D)** Western blot analysis showing digitonin lysates from stable T2 transfectants using antibodies recognizing TAP1 (R.RING4C), Grp94 (9G10), and

TAP2 (K0137-3) (C). Band intensities were determined densitometrically and are expressed as TAP2:TAP1 ratios in a bar diagram (D). **E)** RT-PCR using actin- or TAP2-specific primers. **F, G)** Flow cytometry analysis of surface-HLA-B,C expression using antibody 4E in the indicated T2 transfectants. Results were gated on living, propidium iodide-negative cells (F). Flow cytometry results showing the averages of three independent experiments including the one depicted in Fig. 8F are shown as a bar diagram (G). The error bars are showing the standard deviation from the mean. Statistical analysis was performed by a repeated measures ANOVA test followed by Dunnett's post-test using Prism 4.0 (GraphPad Software) (NS, not significant). **H, I)** Western blot analysis showing digitonin lysates from stable T2 transfectants using antibodies recognizing TAP1 (R.RING4C), Grp94 (9G10), and TAP2 (K0137-3) (H). Band intensities were determined densitometrically and are expressed as TAP2:TAP1 ratios in a bar diagram (I). **J)** RT-PCR using actin- or TAP2-specific primers.

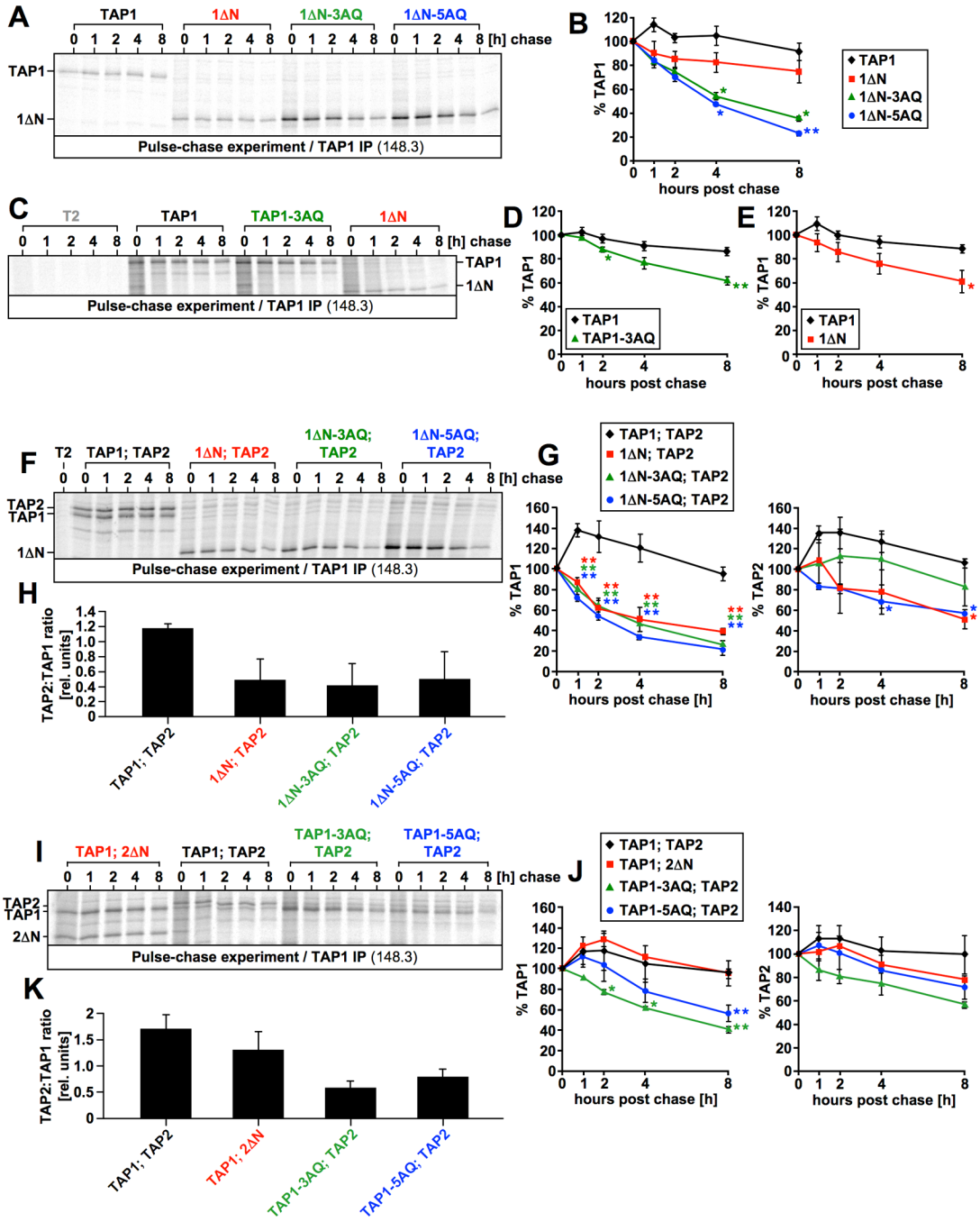

Figure 9. Assembled and unassembled TAP requires tapasin binding for full stability

A–J) Pulse-chase experiments assessing the stability of unassembled TAP1 single chains (A–E) and assembled TAP (F-J). The indicated T2 transfectants were pulse-labeled for 1h with ^{35}S and subsequently chased for up to eight hours. Digitonin lysates derived from the respective cells were immunoprecipitated with the TAP1-specific antibody 148.3, eluted by vortexing in 0.5% SDS at RT and analyzed by autoradiography (A, C, F, I). Quantitative PhosphorImager analysis of the pulse-chase data (0h time-point set to 100%) is shown (B, D, F, G, J). Fig. 9B, 9D, 9E, and the left panels in Fig. 9G and 9J display TAP1, whereas the right panels in Fig. 9G and 9J display TAP2. The error bars in all panels are showing the standard error of the mean. Fig. 9B displays the averages of three independent experiments

including the one depicted in Fig. 9A. Fig. 9D displays the averages of five independent experiments including the one depicted in Fig. 9C. Fig. 9E displays the averages of seven independent experiments including the one depicted in Fig. 9C. The data of the seven experiments depicted in Fig. 9E includes the three experiments shown in Fig. 9B. Fig. 9G displays the averages of three independent experiments including the one depicted in Fig. 9F. Fig. 9J displays the averages of three independent experiments including the one depicted in Fig. 9I. Statistical analysis using Prism 4.0 (GraphPad Software) was carried out on the values from each time-point, normalized in a way that the 0h time-point is set to 100%. For Fig. 9B, statistical analysis was performed by a repeated measures ANOVA test followed by Dunnett's post-test (comparing results against 1ΔN) (* indicates $p < 0.05$, ** indicates $p < 0.01$). For Fig. 9D, statistical analysis was performed by a Two-Tailed Paired t test (* indicates $p = 0.0370$, ** indicates $p = 0.0024$). For Fig. 9E, statistical analysis was performed by a Two-Tailed Paired t test (* indicates $p = 0.0329$). For Fig. 9G and 9J, statistical analysis was performed by a repeated measures ANOVA test followed by Dunnett's post-test (comparing results against TAP1; TAP2) (* indicates $p < 0.05$, *** indicates $p < 0.01$). Fig. 9H and 9K show the non-normalized TAP2:TAP1 ratio at time-point 0h for the experiments depicted in Fig. 9F/G and 9I/J, respectively.